Self-consistent description of local density dynamics in simple liquids. The case of molten lithium

IOP Publishing Journal of Physics: Condensed Matter
J. Phys.: Condens. Matter **30** (2018) 085102 (17pp) https://doi.org/10.1088/1361-648X/aaa7bc

Self-consistent description of local density dynamics in simple liquids. The case of molten lithium

A V Mokshin and B N Galimzyanov

Department of Computational Physics, Institute of Physics, Kazan Federal University, 420008 Kazan, Russia

E-mail: anatolii.mokshin@mail.ru

Received 13 October 2017, revised 6 January 2018
Accepted for publication 15 January 2018
Published 5 February 2018

Abstract

The dynamic structure factor is the quantity, which can be measured by means of Brillouin light-scattering as well as by means of inelastic scattering of neutrons and x-rays. The spectral (or frequency) moments of the dynamic structure factor define directly the sum rules of the scattering law. The theoretical scheme formulated in this study allows one to describe the dynamics of local density fluctuations in simple liquids and to obtain the expression of the dynamic structure factor in terms of the spectral moments. The theory satisfies all the sum rules, and the obtained expression for the dynamic structure factor yields correct extrapolations into the hydrodynamic limit as well as into the free-particle dynamics limit. We discuss correspondence of this theory with the generalized hydrodynamics and with the viscoelastic models, which are commonly used to analyze the data of inelastic neutron and x-ray scattering in liquids. In particular, we reveal that the postulated condition of the viscoelastic model for the memory function can be directly obtained within the presented theory. The dynamic structure factor of liquid lithium is computed on the basis of the presented theory, and various features of the scattering spectra are evaluated. It is found that the theoretical results are in agreement with inelastic x-ray scattering data.

Keywords: microscopic dynamics, liquids, liquid metals, density fluctuations

(Some figures may appear in colour only in the online journal)

1. Introduction

The collective dynamics in a liquid occur over a wide range of spatial scales varied from those comparable with the particle sizes (of the order of few Angstroms) up to macroscopic scales typical for hydrodynamics. The features of these dynamics determine directly the lineshape of the dynamic structure factor $S(k,\omega)$. The long-wavelength limit ($k \to 0$) corresponds to ordinary hydrodynamics, and the spectrum of the dynamic structure factor $S(k,\omega)$ at extremely small values of the wavenumber k is characterized by the line shape known as the Rayleigh–Mandelshtam–Brillouin triplet. This spectrum consists of one central (Rayleigh) peak located at $\omega = 0$ and two side (Brillouin) peaks located at frequencies $\pm\omega_c$, where $\omega_c = c_s k$ and c_s is the adiabatic sound velocity. Hence, the lineshape of $S(k,\omega)$ represents a result of the sum of three Lorentzians (in respect to the frequency ω) [1]:

$$S(k,\omega) = \frac{S(k)}{2\pi}\left\{\left(\frac{\gamma-1}{\gamma}\right)\frac{2D_T k^2}{\omega^2 + (D_T k^2)^2} + \frac{1}{\gamma}\sum_{l=1}^{2}\frac{\Gamma k^2}{[\omega + (-1)^l c_s k]^2 + (\Gamma k^2)^2}\right\}, \quad (1)$$

with the following parameters—the thermal diffusivity D_T, the sound attenuation coefficient $\Gamma = (1/2)[(\gamma-1)D_T + \eta_L]$, the ratio of the specific heat at constant pressure to the specific heat at constant volume $\gamma = c_p/c_V$, the longitudinal viscosity η_L, and the static structure factor $S(k)$. Note that equation (1)

reproduces the next peculiarities of the density fluctuations dynamics observed in the Brillouin light-scattering experiments: (i) the three peaks corresponding to these Lorentzians are well defined and separated by two gaps of the same width; the Rayleigh component $I_{\rm R}$ and the Brillouin component $I_{\rm B}$ are defined as follows

$$I_{\rm R} = \frac{S(k)}{\pi}\left(\frac{\gamma-1}{\gamma}\right)\int_{-\infty}^{\infty}\frac{D_T k^2}{\omega^2+(D_T k^2)^2}\,{\rm d}\omega = S(k)\left(\frac{\gamma-1}{\gamma}\right)$$

and

$$I_{\rm B} = \frac{S(k)}{2\pi}\frac{1}{\gamma}\int_{-\infty}^{\infty}\frac{\Gamma k^2}{[\omega\pm(c_s k)]^2+(\Gamma k^2)^2}\,{\rm d}\omega = \frac{S(k)}{2}\frac{1}{\gamma}. \quad (2)$$

The correspondence between the components is defined by the Landau–Placzek ratio [2]

$$\frac{I_{\rm R}}{2I_{\rm B}} = \gamma - 1; \quad (3)$$

(ii) these peaks are broaden with increase of the wavenumber in accordance with k^2-dependence; and (iii) shift of two symmetric peaks to higher frequencies with increase of the wavenumber k defines the linear low-k asymptotic of the longitudinal sound dispersion, $\lim_{k\to 0}\omega_c(k) = c_s k$.

The Brillouin light-scattering in liquids probes the macroscopical longitudinal density fluctuations. Then, inelastic neutron scattering (INS) and inelastic x-ray scattering (IXS) experiments allow one to extract information about the local density fluctuations corresponding to the microscopic spatial scales with the wavelengths raised by collective dynamics of a few amount of particles up to the wavelengths corresponding to free-particle dynamics regime [3]. Let k_m be the wavenumber corresponding to the first (principal) maximum of the static structure factor $S(k)$. For the case of monatomic liquids, the maximum of the static structure factor, $S(k_m)$, is the largest one, and the quantity $r_m = 2\pi/k_m$ will provide an approximate estimate of an equilibrium distance between the centers of two neighboring atoms. The wavenumbers available via INS and IXS experiments cover a wide range, which includes $k \in [0.1;\ 5]\ k_m$. These experiments have revealed that the three-peak lineshape of $S(k,\omega)$-spectra similar to the Rayleigh–Mandelshtam–Brillouin triplet appears also at finite wavenumbers until the boundary of the first Brillouin pseudozone with $k = k_m/2$, albeit these peaks are not separated, and the experimental $S(k,\omega)$-spectra are not reproducible by equation (1) [4, 5]. With further increase of the wavenumber k, the side peaks of the dynamic structure factor spectra start to shift to the lower frequencies and these peaks disappear completely at $k \simeq 0.75\ k_m$. At these wavenumbers, the tangent to the dispersion curve $\omega_c(k)$ takes a negative slope and the intensity of the central spectral component, $S(k,\omega=0)$, grows. Such changes of the scattering spectra occur until the wave number approaches the value k_m, at which the spectrum of the dynamic structure factor will be represented by the central Rayleigh component. Thus, at the wavenumbers comparable with k_m, the $S(k,\omega)$ spectrum covers a narrow frequency range. This is known as the de Gennes narrowing effect [6, 7]. Further, the wavenumbers $k \geqslant k_m$ correspond to the transition range in the regime of free-particle dynamics. Thus, at very large wavenumbers $k > k_m$, the characteristic wavelengths are shorter than an interparticle distance. Here, the dynamic structure factor $S(k,\omega)$ is reproduced by the Gaussian function

$$S(k,\omega) = \sqrt{\frac{1}{2\pi}}\frac{1}{v_T k}\exp\left(-\frac{\omega^2}{2(v_T k)^2}\right), \quad (4)$$

where v_T is particle velocity.

INS and IXS spectra for the extended wavenumber range $k \in [0.1;\ 1]k_m$ provide a useful information to develop and to test the theoretical models of local density fluctuations dynamics in liquids. The theoretical analysis of these experimental data is usually performed within the time correlation functions (TCF's) formalism [8] and on the basis of ideas of the generalized hydrodynamics [9]. At the present time, there are various theoretical models of the dynamic structure factor $S(k,\omega)$ of simple liquids (for details see reviews [4, 10, 11]). And, as it turned out, it is not difficult to develop a theoretical scheme with a certain amount of adjustable parameters. Nevertheless, the main difficulty here is to propose a theoretical methodology that will ensure the correct transition from hydrodynamic description with a set of macroscopic parameters to description of microscopic dynamics with appropriate characteristics such as the interparticle interaction, the particle velocities and the particle distribution functions. Moreover, a suggested theoretical model has to provide the correct time dependence of the TCFs and has to satisfy the so called sum-rules of a spectral functions [12].

In this work, we will demonstrate that description of density fluctuations dynamics as well as analysis of INS and IXS data of simple liquids can be done self-consistently in terms of the low-order frequency moments (or the low-order frequency parameters) of the dynamic structure factor. In fact, this theoretical scheme formalizes the idea of a self-consistent description of the density fluctuations in the same manner as this is realizing by the mode-coupling theory, where the statistical treatment of the dynamics of a system with an infinite number of degrees of freedom is reduced to closed integro-differential equations [13]. As follows from the theoretical definitions, the frequency moments are related to the microscopic characteristics: the particle interaction energy, the particle velocity, the local structure parameters. This theoretical scheme allows one to obtain the model for the dynamic structure factor of simple liquids.

Liquid alkali metals are suitable candidates to test the proposed theories of the microscopical collective dynamics in a liquid [8, 9, 12, 14]. The potential energy of these systems can be regarded as a quantity determined mainly by the ion-ion interactions, whilst the electron screening effects are taken into account effectively. The interactions between the particles (ions) in alkali metals are reproduced by a potential $u(\mathbf{r})$, which is the simplest in comparison with the potentials for other metals. Therefore, various characteristics of the density fluctuation dynamics in liquid alkali metals can be evaluated on the basis of the proposed microscopic theories, where the

potential is the main input parameter. Note that experimental data for liquid alkali metals [15], including recent results of inelastic neutron and x-ray scattering [3, 10, 11, 16–21], provides a reliable basis for theoretical and numerical simulation studies [22–33].

Liquid lithium has the simple electronic structure $1s^2 2s$ and is characterized by a large ratio of valence electrons to core electrons. This ratio is larger even than for other liquid alkali metals. As a result, some physical properties of lithium determined by the microscopic dynamics turn out to be specific. In particular, liquid lithium has the largest sound velocity and the smallest heat capacity in comparison with other alkalis. Namely, the sound velocity is $c_s = 4554$ m s^{-1} and the molar heat capacity at constant pressure is $c_p = 30.33$ J (mol K)$^{-1}$, whereas the ratio of specific heats $\gamma = c_p/c_V = 1.065$ at the melting temperature $T_\mathrm{m} = 453$ K and ambient pressure [15]. The local and non-local pseudopotentials as well as the more sophisticated EAM and modified EAM (MEAM) potentials have been proposed for the case of liquid lithium. To examine these potentials, the structure and dynamical properties had been evaluated in works of Kresse [34], Canales *et al* [24], Torcini *et al* [22], Gonzalez *et al* [35], Anta and Madden [31], Salmon *et al* [36] and others. It was found that the spectra of the dynamic structure factor obtained by means of molecular dynamics with a pair pseudopotential have better agreement with IXS data than simulation results with the EAM potentials [35, 37]. In addition, many various theoretical models of the dynamic structure factor were tested with the high quality IXS data for liquid lithium [22, 38, 39]. Therefore, we examine our theoretical scheme for the case of liquid lithium.

The paper is organized as follows. Theoretical description is given in section 2. Namely, the basic points and definitions of the time correlation functions formalism are presented in section 2.1. The self-consistent theory of the density fluctuations dynamics in simple liquids developed in the framework of this formalism is presented in section 2.2. In this Subsection, we present the original theoretical results related with the detailed derivation of the expressions for the dynamic structure factor, dispersion relation for the longitudinal collective excitations and other spectral characteristics. Comparison with other theoretical schemes is given in section 3. We discuss the correspondence of our theoretical scheme with the known simple and extended viscoelastic models in section 3.1, with the ordinary and generalized hydrodynamic theories in sections 3.2 and 3.3 and with the model for the free-particle dynamics in section 3.4. In section 4, the theoretical model is applied to compute the dynamic structure factor of liquid lithium and the theoretical results are compared with experimental IXS data for this liquid metal. The concluding remarks are given in section 5.

2. Theoretical description

2.1. Fundamental notions

According to statistical mechanics, if one treats an equilibrium liquid as a many-particle system, then it is convenient to apply the mathematical formalism of the correlation functions, distribution functions, the moments and cumulants of these functions. In particular, the time correlation functions allow us to describe the relaxation processes occurring in the system at different spatial scales [40]. As a result, the corresponding microscopic theory can be developed. In the given study, we are focused on the collective particle dynamics of a liquid. Therefore, we assume that the particle interaction potential and such the structural parameters as the particle distribution functions and the static structure factor are defined and can be used as input parameters of the theoretical scheme.

Let us consider an isotropic system, which consists on N classical particles of a mass m enclosed in a volume V. As an initial dynamical variable we take the Fourier-component of the local density fluctuations

$$\rho_k = \frac{1}{\sqrt{N}} \sum_{j=1}^{N} \mathrm{e}^{\mathrm{i}\mathbf{k}\cdot\mathbf{r}_j}, \quad k = |\mathbf{k}|, \tag{5}$$

whose evolution is defined by the corresponding equation of motion

$$\dot{\rho}_k(t) = \mathrm{i}\hat{\mathcal{L}}\rho_k(t). \tag{6}$$

Here, the dot denotes time differentiation, and $\hat{\mathcal{L}}$ is the Liouville operator, which is Hermitian [40, 41]:

$$\hat{\mathcal{L}} = -\mathrm{i}\left\{ \frac{1}{m}\sum_{j=1}^{N}(\mathbf{p}_j \cdot \nabla_j) - \sum_{l>j=1}^{N} \nabla_j u(r_{jl}) \left(\nabla_{\mathbf{p}_j} - \nabla_{\mathbf{p}_l}\right) \right\}. \tag{7}$$

Further, $\mathbf{p}_j$ is the momentum of the jth particle, ∇_j and $\nabla_{\mathbf{p}_j}$ are the gradients over coordinates and momenta, respectively. The quantity $u(r)$ is the interaction energy between a pair of the particles and, as expected, it can be evaluated from any model potential. By means of the Gram–Schmidt orthogonalization procedure [42] on the basis of the quantity $A_0(k) \equiv \rho_k$ we generate the infinite set of variables

$$\mathbf{A}(k) = \{A_0(k),\ A_1(k),\ A_2(k),\ \ldots\} \tag{8}$$

related by

$$\begin{aligned} &A_{j+1}(k) = \mathrm{i}\hat{\mathcal{L}}A_j(k) + \Delta_j^2(k)A_{j-1}(k), \\ &j = 0,\ 1,\ 2,\ \ldots; \\ &A_{-1} \equiv 0. \end{aligned} \tag{9}$$

Here,

$$\Delta_{j+1}^2(k) = \frac{\langle |A_{j+1}(k)|^2 \rangle}{\langle |A_j(k)|^2 \rangle} \tag{10}$$

is an jth-order frequency parameter (at fixed k), which has a dimension of square frequency [43]; and the brackets $\langle \ldots \rangle$ denote the ensemble average.

The variables of set (8) are the generalized dynamical variables dependent on the wavenumber k as parameter (see discussion in [44], pp 100–1). These variables form an orthogonal basis [41, 42]:

$$\begin{aligned} &\langle A_i^*(k)A_j(k)\rangle = \delta_{i,j}\langle |A_j(k)|^2 \rangle, \\ &i,j = 0,\ 1,\ 2,\ \ldots. \end{aligned} \tag{11}$$

Further, while the first variable $A_0(k)$ is defined by equation (5), then the second variable is

$$A_1(k) = \frac{\mathrm{i}}{\sqrt{N}} \sum_{j=1}^{N} (\mathbf{k}\cdot\mathbf{v}_j)\mathrm{e}^{\mathrm{i}\mathbf{k}\cdot\mathbf{r}_j}, \tag{12}$$

and for the third variable one has

$$\begin{aligned} A_2(k) &= \dot{A}_1(k) + \Delta_1^2(k)A_0(k) \\ &= -\frac{1}{\sqrt{N}} \sum_{j=1}^{N} (\mathbf{k}\cdot\mathbf{v}_j)^2 \,\mathrm{e}^{\mathrm{i}\mathbf{k}\cdot\mathbf{r}_j} \\ &\quad + \frac{\mathrm{i}}{\sqrt{mN}} \sum_{l>j=1}^{N} (\nabla_j\cdot\mathbf{k})u(r_{jl}) \left\{\mathrm{e}^{\mathrm{i}\mathbf{k}\cdot\mathbf{r}_j} - \mathrm{e}^{\mathrm{i}\mathbf{k}\cdot\mathbf{r}_l}\right\} + \Delta_1^2(k)A_0(k). \end{aligned} \tag{13}$$

Let us define the TCF

$$M_j(k,t) = \frac{\langle A_j^*(0)A_j(t)\rangle}{\langle |A_j^*(0)|^2\rangle}, \quad j = 0,\ 1,\ 2,\ \ldots, \tag{14}$$

which will be characterized by the properties

$$M_j(k,t)|_{t=0} = 1, \tag{15a}$$

$$|M_j(k,t)| \leqslant 1, \tag{15b}$$

and

$$\left.\frac{\mathrm{d}^l}{\mathrm{d}t^l}M_j(k,t)\right|_{t=0} = 0, \quad \text{if } l \text{ is odd},$$
$$\left.\frac{\mathrm{d}^l}{\mathrm{d}t^l}M_j(k,t)\right|_{t=0} \neq 0, \quad \text{if } l \text{ is even}. \tag{15c}$$

These properties are directly derived from condition (11). Then, the TCF

$$M_0(k,t) = F(k,t) = \frac{\langle \rho_k^*(0)\rho_k(t)\rangle}{\langle |\rho_k(0)|^2\rangle} \tag{16}$$

represents the density–density correlation function known also as the intermediate scattering function. This TCF is related to the dynamic structure factor [8]

$$S(k,\omega) = \frac{S(k)}{2\pi}\int_{-\infty}^{\infty} \exp(\mathrm{i}\omega t)F(k,t)\,\mathrm{d}t, \tag{17}$$

where $S(k) = \langle|\rho_k(0)|^2\rangle$ is the static structure factor. Taking into account property (15c), one obtains the short-time expansion for the intermediate scattering function:

$$F(k,t) = 1 - \langle\omega^{(2)}(k)\rangle\frac{t^2}{2!} + \langle\omega^{(4)}(k)\rangle\frac{t^4}{4!} + \ldots + (-\mathrm{i})^l\langle\omega^{(l)}(k)\rangle\frac{t^l}{l!} + \ldots,$$

where $\langle\omega^{(l)}\rangle$ is the lth-order normalized frequency moment of the dynamic structure factor $S(k,\omega)$ [45–49]:

$$\langle\omega^{(l)}(k)\rangle = (-\mathrm{i})^l\left.\frac{\mathrm{d}^{(l)}}{\mathrm{d}t^l}F(k,t)\right|_{t=0} = \frac{\int_{-\infty}^{\infty}\omega^l S(k,\omega)\mathrm{d}\omega}{\int_{-\infty}^{\infty}S(k,\omega)\mathrm{d}\omega}. \tag{18}$$

The quantity $M_1(k,t)$ is the TCF associated with the longitudinal-current autocorrelation function

$$C_L(k,t) = \frac{\langle j_k^{(L)}(0)j_k^{(L)}(t)\rangle}{\langle|j_k^{(L)}(0)|^2\rangle}, \tag{19}$$

which is related, in turn, to the intermediate scattering function $F(k,t)$ as follows [14]

$$-\frac{\mathrm{d}^2}{\mathrm{d}t^2}F(k,t) = \Delta_1^2(k)C_L(k,t). \tag{20}$$

The label L denotes the component parallel to the wavevector $\mathbf{k}$. Relation (20) is direct consequence of the *hydrodynamic* continuity equation

$$\frac{\partial}{\partial t}\rho_k(t) + \mathrm{i}kj_k^{(L)} = 0, \tag{21}$$

which shows that spontaneous fluctuations of a conserved *hydrodynamic* variable $\rho_k(t)$ decay very slowly at long wavelengths (i.e. at extremely small wavenumbers) [8]. Then, taking into account equation (17) one obtains the correspondence between the spectral density of the longitudinal-current fluctuations

$$C_L(k,\omega) = \frac{1}{2\pi}\int_{-\infty}^{\infty}\exp(\mathrm{i}\omega t)C_L(k,t)\,\mathrm{d}t$$

and the dynamic structure factor $S(k,\omega)$ [50, 51]:

$$S(k)\Delta_1^2(k)C_L(k,\omega) = \omega^2 S(k,\omega). \tag{22}$$

Further, from equation (13) one can verify that the TCF $M_2(k,t)$ is expressed in terms of the TCFs of energy or stress tensor, of force and of density as well as in terms of the corresponding cross-correlation functions. Then, the TCF $M_3(k,t)$ will contain a contribution related to the TCF of energy current [28]. Thus, the quantities $F(k,t)$, $M_1(k,t)$, $M_2(k,t)$ and $M_3(k,t)$ are the TCFs of the variables arising also in the hydrodynamic conservation laws for the longitudinal collective dynamics. These TCFs correspond to the concrete relaxation processes [52]. The time scales of the relaxation processes can be conveniently evaluated by

$$\tau_j(k) = \frac{1}{\sqrt{\Delta_j^2(k)}}, \quad j = 0,\ 1,\ 2,\ \ldots. \tag{23}$$

The functions $F(k,t)$, $C_L(k,t)$, $M_2(k,t)$ and $M_3(k,t)$ obey the next kinetic integro-differential equations:

$$\ddot{F}(k,t) + \Delta_1^2(k)F(k,t) + \Delta_2^2(k)\int_0^t \mathrm{d}\tau M_2(k,t-\tau)\dot{F}(k,\tau') = 0, \tag{24a}$$

$$\ddot{M}_1(k,t) + \Delta_2^2(k)M_1(k,t) + \Delta_3^2(k)\int_0^t \mathrm{d}\tau M_3(k,t-\tau)\dot{M}_1(k,\tau') = 0, \tag{24b}$$

$$\ddot{M}_2(k,t) + \Delta_3^2(k)M_2(k,t) + \Delta_4^2(k)\int_0^t \mathrm{d}\tau M_4(k,t-\tau)\dot{M}_2(k,\tau') = 0. \tag{24c}$$

Equations (24a)–(24c) can be derived by means of the recurrent relations method [42] or by the projection operators technique [40] from the equations of motion for the variables $A_0(k)$, $A_1(k)$ and $A_2(k)$. Recall that the frequency parameters

$\Delta_1^2(k)$, $\Delta_2^2(k)$, $\Delta_3^2(k)$ and $\Delta_4^2(k)$ can be found directly from definition (10). On the other hand, one obtains from (18) that

$$\Delta_1^2(k) = \langle\omega^{(2)}(k)\rangle, \tag{25a}$$

$$\Delta_2^2(k) = \frac{\langle\omega^{(4)}(k)\rangle}{\langle\omega^{(2)}(k)\rangle} - \langle\omega^{(2)}(k)\rangle, \tag{25b}$$

$$\Delta_3^2(k) = \frac{\langle\omega^{(6)}(k)\rangle\langle\omega^{(2)}(k)\rangle - (\langle\omega^{(4)}(k)\rangle)^2}{\langle\omega^{(4)}(k)\rangle\langle\omega^{(2)}(k)\rangle - (\langle\omega^{(2)}(k)\rangle)^3}, \tag{25c}$$

$$\Delta_4^2(k) = \frac{1}{\Delta_1^2(k)\Delta_2^2(k)\Delta_3^2(k)}\Big\{\langle\omega^{(8)}(k)\rangle - \Delta_1^2(k)\Big[\Big(\Delta_1^2(k)+\Delta_2^2(k)\Big)^3 + 2\Delta_2^2(k)\Delta_3^2(k)\Big(\Delta_1^2(k)+\Delta_2^2(k)\Big) + \Delta_2^2(k)\Delta_3^4(k)\Big]\Big\}, \tag{25d}$$

$$\Delta_5^2(k) = \frac{1}{\Delta_1^2(k)\Delta_2^2(k)\Delta_3^2(k)\Delta_4^2(k)}\Big\{\omega^{(10)}(k) - \Delta_1^2(k)\Big[\Big(\Delta_1^2(k)+\Delta_2^2(k)\Big)^2 + \Delta_2^2(k)\Delta_3^2(k)\Big]^2 - \Delta_1^2(k)\Delta_2^2(k)\Delta_3^2(k)\Big[\Delta_1^2(k)+\Delta_2^2(k)+\Delta_3^2(k)+\Delta_4^2(k)\Big]^2\Big\}. \tag{25e}$$

One can see that the frequency parameter of the jth order is defined through the frequency moments up to the moment of the $2j$th order. Relations similar to (25*a*)–(25*e*) can be also written for the frequency parameters of the higher order. Moreother, relations (18), (25*a*)–(25*e*) are the low-order sum rules of the scattering law $S(k,\omega)$.

Taking into account the statistical average in the product of the dynamical variables in relation (10), the frequency moments $\langle\omega^{(l)}(k)\rangle$ can be expressed in terms of the thermal velocity $v_{\rm th} = \sqrt{k_{\rm B}T/m}$ of a particle, the interparticle potential $u(\mathbf{r})$ and the particles distribution functions. Thus, the first frequency parameter $\Delta_1^2(k)$ is defined as

$$\Delta_1^2(k) = \frac{k_{\rm B}T}{m}\frac{k^2}{S(k)} = \frac{(v_{\rm th}k)^2}{S(k)}. \tag{26a}$$

The second frequency parameter $\Delta_2^2(k)$ can be found from

$$\Delta_2^2(k) = 3\frac{k_{\rm B}T}{m}k^2 - \Delta_1^2(k) + \frac{\rho}{m}\int\nabla_l^2 u(\mathbf{r})[1-\exp(\mathrm{i}\mathbf{k}\cdot\mathbf{r})]g(r)\mathrm{d}^3\mathbf{r} \approx 3\left(\frac{k_{\rm B}T}{m}k^2+\omega_E^2\right) - \Delta_1^2(k) - \frac{\rho}{m}\int\nabla_l^2 u(\mathbf{r})\exp(\mathrm{i}\mathbf{k}\cdot\mathbf{r})g(r)\mathrm{d}^3\mathbf{r}. \tag{26b}$$

The third frequency parameter is defined as

$$\Delta_3^2(k) = \frac{1}{\Delta_2^2(k)}\left\{15\left(\frac{k_{\rm B}T}{m}k^2\right)+\mathcal{F}(k)\right\} - \frac{1}{\Delta_2^2(k)}\left[\Delta_1^2(k)+\Delta_2^2(k)\right]^2. \tag{26c}$$

Here, $\rho = N/V$ is the number density, $g(r)$ is the pair distribution function, ω_E is the so-called Einstein frequency, and the term $\mathcal{F}(k)$ denotes the combination integral expressions containing the interparticle potential $u(\mathbf{r})$ and such the structural characteristics as the two- and three-particle distribution functions [32]. Moreover, the jth order relaxation parameter $\Delta_j^2(k)$ with $j \geqslant 2$ will be defined by the potential $u(\mathbf{r})$ as well as by the distribution functions of two, three, …, $(j-2)$, $(j-1)$ and j particles. Thus, the relaxation parameters $\Delta_j^2(k)$ at $j \geqslant 2$ are directly dependent on the type of interaction between the particles and on the microscopic structural characteristics.

Equation (24*a*) is also known as the generalized Langevin equation. By the Laplace transformation

$$LT\{f\}(s) = \tilde{f}(s) = \int_0^\infty \mathrm{e}^{-st}f(t)\,\mathrm{d}t, \qquad s = \mathrm{i}\omega,$$

of equation (24*a*) and solving it in terms of equation (17), one obtains expression for the *classical* dynamic structure factor:

$$S(k,\omega) = \frac{S(k)}{\pi}\frac{\Delta_1^2(k)\Delta_2^2(k)M_2'(k,\omega)}{[\omega^2-\Delta_1^2(k)+\omega\Delta_2^2(k)M_2''(k,\omega)]^2+[\omega\Delta_2^2(k)M_2'(k,\omega)]^2}, \tag{27}$$

where $\widetilde{M}_2'(k,\omega)$ and $\widetilde{M}_2''(k,\omega)$ are the real and imaginary parts of $\widetilde{M}_2(k, s=\mathrm{i}\omega)$, respectively. Equation (27) is usually applied to explain the features of the experimental dynamic structure factor [4]. This implies in fact a fitting of the experimental $S(k,\omega)$ by equation (27) with a suggested theoretical model for the TCF $M_2(k,t)$ [8]. In particular, if the TCF decays instantaneously, $M_2(k,t) = \tau_2(k)\delta(t)$, then equation (27) reduces to the equation for the *damped harmonic oscillator* (DHO) model:

$$S(k,\omega) = \frac{S(k)}{\pi}\frac{\Delta_1^2(k)\Delta_2^2(k)\tau_2(k)}{[\omega^2-\Delta_1^2(k)]^2+[\omega\Delta_2^2(k)\tau_2(k)]^2}, \tag{28}$$

where $\tau_2(k)$ is the damping parameter. On the other hand, the TCF with an exponential decay

$$M_2(k,t) = \mathrm{e}^{-t/\tau_2(k)} \tag{29}$$

yields the *simple viscoelastic model* for the dynamic structure factor $S(k,\omega)$ [5].

2.2. Self-consistent approach

The equations similar to kinetic equations (24*a*)–(24*c*) can be written for the TCF's of other dynamical variables—$M_3(k,t)$, $M_4(k,t)$, …, $M_j(k,t)$, …. As a result, one obtains the infinite chain of the connected equations [8]. Applying the Laplace transform to these equations, one obtains a continued fraction representation for the Laplace transform of the intermediate scattering function $\widetilde{F}(k,s)$:

$$\widetilde{F}(k,s) = \cfrac{1}{s+\Delta_1^2(k)\widetilde{M}_1(k,s)} = \cfrac{1}{s+\cfrac{\Delta_1^2(k)}{s+\cfrac{\Delta_2^2(k)}{s+\cfrac{\Delta_3^2(k)}{s+\ddots}}}}. \tag{30}$$

This fraction indicates that the dynamic structure factor

$$S(k,\omega) = \frac{S(k)}{\pi}\mathrm{Re}[\widetilde{F}(k,s=\mathrm{i}\omega)] \tag{31}$$

is directly defined by the frequency parameters $\Delta_j^2(k)$'s and, thereby, by the dynamical variables of set (8). Estimation of the low-order frequency parameters for liquid metals (cesium [26, 27], sodium [28, 29], aluminum [28, 30, 33]) sets the following regularity:

$$\Delta_{j+1}^2(k) \geqslant \Delta_j^2(k), \qquad j = 1,\ 2,\ 3,\ \ldots, \quad k \text{ is fixed.} \tag{32}$$

This is evidence that the relaxation process associated with a higher-order dynamical variable takes place on a shorter time-scale [52][1]. Then, one can reasonably expect for the high-order frequency parameters starting from the parameter with a some index ξ that

$$\Delta_\xi^2(k) \gg \omega^2, \qquad \xi \text{ is natural number,} \tag{33}$$

where ω's are the inherent frequencies of the relaxation processes associated with the density fluctuations. These frequencies ω correspond to the range (at the given k), where the inelastic components of $S(k,\omega)$ are observed. This means that the time scale of density fluctuations $\tau_\alpha(k) \propto 1/\sqrt{\Delta_1^2(k)}$ is much larger than the associated time scales $\tau_\xi(k) = 1/\sqrt{\Delta_\xi^2(k)}$, $\tau_{\xi+1}(k) = 1/\sqrt{\Delta_{\xi+1}^2(k)}$ and so on. Then, assuming that the time scales take small but still finite values one can write that

$$\Delta_\xi^2(k) = \Delta_{\xi+1}^2(k) = \Delta_{\xi+2}^2(k) = \ldots. \tag{34}$$

Condition (34) has the important inferences.

(i) This condition corresponds exactly to the TCF $M_{\xi-1}(k,t)$ with the following time dependence [43]:

$$M_{\xi-1}(k,t) = \frac{1}{\sqrt{\Delta_\xi^2(k)t}} J_1\left(2\sqrt{\Delta_\xi^2(k)t}\right). \tag{35}$$

The Laplace transform of this TCF is

$$\widetilde{M}_{\xi-1}(k,s) = \frac{-s + [s^2 + 4\Delta_\xi^2(k)]^{1/2}}{2\Delta_\xi^2(k)}. \tag{36}$$

Here, $J_1(x)$ is the Bessel function of the first kind. As a result, the frequency dependence of all the quantities, $\widetilde{F}(k,s)$, $\widetilde{M}_1(k,s)$, $\widetilde{M}_2(k,s)$, …, $\widetilde{M}_{\xi-2}(k,s)$, can be recovered by substitution of (36) into fraction (30).

(ii) Condition (34) is equivalent to equality of the TCFs [43]:

$$M_\xi(k,t) = M_{\xi-1}(k,t), \tag{37}$$

which yields the correspondence between the dynamical variables:

$$A_\xi(k) \sim A_{\xi-1}(k). \tag{38}$$

The physical meaning of (38) is that the set $\mathbf{A}(k)$ (see (8)) reduces to the finite amount of the dynamical variables:

$$A_0(k),\ A_1(k),\ A_2(k),\ \ldots,\ A_{\xi-1}(k). \tag{39}$$

Relation (37) yields directly solution of the chain of integro-differential equations (26) in a self-consistent way similar to that as this is realized in the mode-coupling theories [44].

To be consistent with hydrodynamic theory, the finite set of the dynamical variables has to include, at least, first four dynamical variables of set (8), i.e. $\xi = 4$ in set (39), corresponding to the hydrodynamic variables [8]. Then, (by analogy with equation (36)) one obtains the following s-dependence of $\widetilde{M}_3(k,s)$:

$$\widetilde{M}_3(k,s) = \frac{-s + [s^2 + 4\Delta_4^2(k)]^{1/2}}{2\Delta_4^2(k)}. \tag{40}$$

Further, the Laplace transform $\widetilde{M}_2(k,s) = M_2'(k,\omega) + \mathrm{i}M_2''(k,\omega)$, which appears in general expression (27) for the dynamic structure factor, takes the form

$$\widetilde{M}_2(k,s) = \frac{2\Delta_4^2(k)}{s\left[2\Delta_4^2(k) - \Delta_3^2(k)\right] + \Delta_3^2(k)\sqrt{s^2 + 4\Delta_4^2(k)}}, \tag{41}$$

whereas the dynamic structure factor is

$$S(k,\omega) = \frac{S(k)}{2\pi} \frac{\Delta_1^2(k)\Delta_2^2(k)\Delta_3^2(k)}{\Delta_4^2(k) - \Delta_3^2(k)} \frac{[4\Delta_4^2(k) - \omega^2]^{1/2}}{\omega^6 + \mathcal{A}_1(k)\omega^4 + \mathcal{A}_2(k)\omega^2 + \mathcal{A}_3(k)} \tag{42a}$$

with

$$\mathcal{A}_1(k) = \frac{\Delta_3^4(k) - \Delta_2^2(k)[2\Delta_4^2(k) - \Delta_3^2(k)]}{\Delta_4^2(k) - \Delta_3^2(k)} - 2\Delta_1^2(k),$$

$$\mathcal{A}_2(k) = \frac{\Delta_2^4(k)\Delta_4^2(k) - 2\Delta_1^2(k)\Delta_3^4(k) + \Delta_1^2(k)\Delta_2^2(k)[2\Delta_4^2(k) - \Delta_3^2(k)]}{\Delta_4^2(k) - \Delta_3^2(k)} + \Delta_1^4(k),$$

$$\mathcal{A}_3(k) = \frac{\Delta_1^4(k)\Delta_3^4(k)}{\Delta_4^2(k) - \Delta_3^2(k)}. \tag{42b}$$

Taking into account the condition $4\Delta_4^2(k) \gg \omega^2$, which is equivalent to (33) at $\xi = 4$, the numerator of (42a) turns into product of the frequency parameters $\Delta_1^2(k)$, $\Delta_2^2(k)$, $\Delta_3^2(k)$ and $\Delta_4^2(k)$. Then, the spectral features of the dynamic structure factor spectrum $S(k,\omega)$ at a given k will be defined according to (42a) by the bicubic polynomial (in the variable ω) in the denominator with the coefficients $\mathcal{A}_1(k)$, $\mathcal{A}_2(k)$, $\mathcal{A}_3(k)$. It should be noted that the scattering spectra defined by equation (42a) satisfy all the sum rules.

The fact that the higher order frequency parameters, $\Delta_5^2(k)$, $\Delta_6^2(k)$, …, are not included in expression (42a) for the dynamic structure factor is naturally due to that the relaxation processes associated with such the dynamical variables as the time derivatives of the energy current have no direct influence on the longitudinal density fluctuations dynamics. This is realized when the time scales of these relaxation processes in a liquid are finite, comparable, but much shorter than the time scale of the density fluctuations dynamics. On the other hand,

[1] Increase of parameters $\Delta_j^2(k)$ with growing j is not surprising, because the spectral moment (and, therefore, the corresponding frequency parameter) of a higher order characterizes the spectral features with higher frequencies. Moreover, rigorous inequality $\Delta_{j+1}^2(k) > \Delta_j^2(k)$ at $j = 1$ is well-known for the case of classical liquids (see, for example, on pp 330–1 in review [53]).

applying equation (36) at an arbitrary index $\xi > 4$ to continued fraction (30), expression (42*a*) is modified to the form, which includes $\Delta_5^2(k)$, $\Delta_6^2(k)$, etc. Nevertheless, if these high-order frequency parameters have approximately equal values, then the modified expression for the dynamic structure factor will yield the same spectral lineshape as expression (42*a*).

As seen from (42*a*), all the spectral features of the dynamic structure factor $S(k,\omega)$ are directly defined by the interaction potential $u(\mathbf{r})$ and by such the structural characteristics as the distribution functions of two, three and four particles. These quantities appear in expressions for the frequency parameters $\Delta_1^2(k)$, $\Delta_2^2(k)$, $\Delta_3^2(k)$ and $\Delta_4^2(k)$. The distribution functions of larger amount of particles do not appear in this theoretical model. Finally, it is necessary to note that no assumptions about amount of relaxation modes and about their time/frequency dependencies were made to obtain expression (42*a*) for the dynamic structure factor.

Moreover, analysis of (42*a*) reveals that the dynamic structure factor $S(k,\omega)$ at fixed k must be also characterized by three peaks located at

$$\omega_0 = 0 \quad \text{(central peak)} \tag{43a}$$

and

$$\omega_{+,-}^{(\max)}(k) = \pm\sqrt{\frac{-\mathcal{A}_1(k) + \sqrt{\mathcal{A}_1(k)^2 - 3\mathcal{A}_2(k)}}{3}}$$
$$\text{(high} - \text{frequency doublet)} \tag{43b}$$

as well as by two minima disposed at the frequencies

$$\omega_{+,-}^{(\min)}(k) = \pm\sqrt{\frac{-\mathcal{A}_1(k) - \sqrt{\mathcal{A}_1(k)^2 - 3\mathcal{A}_2(k)}}{3}}. \tag{43c}$$

Note that equations (43*a*)–(43*c*) account for the features of the dynamic structure factor $S(k,\omega)$ at the frequencies $\omega^2 \ll 4\Delta_4^2(k)$. Here, $\omega_{+,-}^{(\max)}(k)$ are the positions of the Brillouin symmetric components in $S(k,\omega)$. The dispersion relation $\omega_m(k) = c_s k$ with the adiabatic sound velocity c_s can be recovered from the maxima of the longitudinal-current spectral density $C_L(k,\omega)$ (see, for instance, analysis of the experimental IXS data given in [10]). Nevertheless, since the longitudinal-current spectral density $C_L(k,\omega)$ is proportional to $\omega^2 S(k,\omega)$, then it is obvious that relation (43*b*) with $\omega_c(k) \equiv \omega_{+,-}^{(\max)}(k)$ will also provide an information about the sound dispersion in a liquid [12]. It is usually expected that both the quantities $\omega_m(k)$ and $\omega_c(k)$ are close at small values of k, and the frequency $\omega_m(k)$ is extrapolated at low-k limit into the frequency of the Brillouin doublet, i.e.

$$\lim_{k\to 0}\sqrt{\frac{-\mathcal{A}_1(k) + \sqrt{\mathcal{A}_1(k)^2 - 3\mathcal{A}_2(k)}}{3}} = c_s k. \tag{44}$$

Further, the values of the frequencies $\omega_m(k)$ and $\omega^{(\max)}(k)$ diverge with increase of the wavenumber k (see discussion on p 304 in [14]).

Taking into account equations (40), (41) and (30), we obtain the dispersion equation:

$$s^3 + \frac{2\Delta_3^2(k)\sqrt{\Delta_4^2(k)}}{2\Delta_4^2(k) - \Delta_3^2(k)}s^2 + \left[\Delta_1^2(k) + \Delta_2^2(k) + \frac{\Delta_2^2(k)\Delta_3^2(k)}{2\Delta_4^2(k) - \Delta_3^2(k)}\right]s + \frac{2\Delta_1^2(k)\sqrt{\Delta_4^2(k)}}{2\Delta_4^2(k) - \Delta_3^2(k)} = 0, \tag{45}$$

which corresponds to the hydrodynamic dispersion equation [54]. Following the convergent Mountain's scheme for approximating solutions [54], we find the correspondence between the hydrodynamic parameters and the frequency parameters for the low-k limit:

$$c_s k = \sqrt{\Delta_1^2(k) + \Delta_2^2(k) + \frac{\Delta_2^2(k)\Delta_3^2(k)}{2\Delta_4^2(k) - \Delta_3^2(k)}}, \tag{46}$$

$$D_T k^2 = \frac{2\Delta_1^2(k)\Delta_3^2(k)\sqrt{\Delta_4^2(k)}}{\Delta_1^2(k)[2\Delta_4^2(k) - \Delta_3^2(k)] + 2\Delta_2^2(k)\Delta_4^2(k)} \tag{47}$$

and

$$\Gamma k^2 = \frac{2\Delta_2^2(k)\Delta_3^2(k)\Delta_4^2(k)\sqrt{\Delta_4^2(k)}}{(2\Delta_4^2(k) - \Delta_3^2(k))[\Delta_1^2(k)(2\Delta_4^2(k) - \Delta_3^2(k)) + 2\Delta_2^2(k)\Delta_4^2(k)]}. \tag{48}$$

Further, according to relation (42*a*), the intensity of the central component of the dynamic structure factor $S(k,\omega)$ spectrum at the fixed wavenumber k is

$$S(k,\omega=0) = \frac{S(k)}{\pi}\frac{\Delta_2^2(k)\sqrt{\Delta_4^2(k)}}{\Delta_1^2(k)\Delta_3^2(k)}. \tag{49}$$

In the hydrodynamic limit ($k \to 0$), this component transforms to the Rayleigh component:

$$S(k,\omega=0) = \frac{S(k)}{\pi}\left(\frac{\gamma-1}{\gamma}\right)\frac{1}{D_T k^2}, \tag{50}$$

which is observed in the Brillouin light-scattering.

3. Comparison with other theoretical schemes

3.1. Extended viscoelastic model

It was revealed in [38, 57] that the three-peak lineshape of $S(k,\omega)$ of liquid metals is well reproduced within the extended viscoelastic model (the so-called 'two relaxation time model' according to terminology of [11, 58]; or 'two-time' viscoelastic model—in the notations of [59]). In this model, the scattering intensity is fitted by equation (27) for the dynamic structure factor with the following approximation for the memory function:

$$\Delta_2^2(k)M_2(k,t) \simeq \sum_{j=D,\alpha,\mu} b_j^2\, \mathrm{e}^{-t/\tau_j(k)},$$
$$b_D^2(k) = (\gamma-1)\Delta_1^2(k), \quad \tau_D(k) = (D_T k^2)^{-1},$$
$$b_\alpha^2 + b_\mu^2(k) = \Delta_L^2(k). \tag{51}$$

Equation (51) is an extension of the simple viscoelastic model [5]. Here, the TCF $M_2(k,t)$ is approximated by the linear

combination of the three exponentially decaying functions responsible for thermal fluctuations

$$m_{\rm th}(k,t) \simeq {\rm e}^{-D_T k^2 t} \tag{52}$$

and for two viscous channels

$$m_L(k,t) \simeq \sum_{j=\alpha,\mu} b_j^2(k)\ {\rm e}^{-t/\tau_j(k)}, \tag{53}$$

where $b_j^2(k)$ and $\tau_j(k)$ are the strengths and the relaxation times of the α and μ viscous regimes, respectively [10]. In the case of liquid alkali metals, the specific-heat ratio $\gamma = c_P/c_V$ takes values comparable with unity [10]. As a result, contribution of the first term (with the label D) in equation (51) to $M_2(k,\ t)$ is negligible. Therefore, the time-dependence of the memory function $M_2(k,\ t)$ and the lineshape of $S(k,\omega)$ will be determined mainly by the parameters of two exponentially decaying functions associated with the viscous modes [11]. One needs to note that there is no guidance or microscopic relations to evaluate the characteristics of the viscous channels. Nevertheless, it was demonstrated [10, 60–62] that this extended viscoelastic model is capable to reproduce the experimental $S(k,\omega)$-spectra within the wavenumber range $k \in [0.1;\ 0.5]\ k_m$ for various liquid metals (not only alkali metals).

Then the following question arises naturally: *is there a correspondence between the theoretical model presented in this work and the extended viscoelastic model?* A simple way to verify a possible correspondence and then to answer this question is to consider equation (41) for the TCF $\widetilde{M}_2(k,s)$ taking the quantity

$$\xi(k) = \left| \frac{s^2}{4\Delta_4^2(k)} \right|$$

as a small parameter. By expanding the radicand in equation (41) over the small parameter ξ:

$$\sqrt{1+\xi(k)} = 1 + \frac{\xi(k)}{2} - \frac{\xi^2(k)}{8} + \ldots, \tag{54}$$

one obtains directly from equation (40) that

$$\widetilde{M}_3(k,s) = -\frac{s}{2\Delta_4^2(k)} + \frac{1}{\sqrt{\Delta_4^2(k)}} + \frac{\xi(k)}{2\sqrt{\Delta_4^2(k)}} - \frac{\xi^2(k)}{8\sqrt{\Delta_4^2(k)}} + \ldots, \tag{55}$$

whereas equation (41) takes the form:

$$\widetilde{M}_2(k,s) \simeq \sum_j \frac{a_j^2(k)}{s+\tau_j^{-1}(k)}, \tag{56}$$

or, equivalently,

$$M_2(k,t) \simeq \sum_j a_j^2(k)\ {\rm e}^{-t/\tau_j(k)}, \qquad \sum_j a_j^2(k) = 1, \qquad j = 1,\ 2,\ 3,\ 5,\ \ldots. \tag{57}$$

Here, the weight coefficients $a_j^2(k)$ and the relaxation times $\tau_j(k)$ are defined through the frequency parameters $\Delta_3^2(k)$ and $\Delta_4^2(k)$. Thus, we obtained in the framework of our theoretical model an approximate expansion of the function $M_2(k,\ t)$ by the exponential contributions. The amount of the Lorentzian functions in (56) and/or the amount of the exponential functions in (57) is determined by the amount of terms taken into account in expansion (54).

For example, assuming that $\xi(k) \to 0$, one obtains

$$\widetilde{M}_3(k,s) \simeq \frac{2\sqrt{\Delta_4^2(k)} - s}{2\Delta_4^2(k)} \tag{58}$$

and

$$\widetilde{M}_2(k,s) \simeq \frac{1}{s+\tau^{-1}(k)}, \quad M_2(k,t) \simeq {\rm e}^{-t/\tau(k)} \tag{59}$$

with the relaxation time

$$\tau^{-1}(k) \simeq \frac{2\sqrt{\Delta_4^2(k)}\Delta_3^2(k)}{2\Delta_4^2(k) - \Delta_3^2(k)}. \tag{60}$$

Equation (59) is equivalent to (29) and corresponds to the *simple viscoelastic model* [5].

Further, expansion (57) at $j = 3$ is similar to the *extended viscoelastic model* with the memory function $M_2(k,\ t)$ represented by equation (51). The inverse relaxation times for this case can be estimated as follows

$$\tau_{\alpha,\mu}^{-1}(k) \simeq \sqrt{\Delta_4^2(k)} \pm \sqrt{\Delta_4^2(k) - \Delta_3^2(k)}, \tag{61}$$

whereas the weight coefficient (say, for the αth contribution) is

$$b_\alpha^2(k) \simeq \frac{1}{2} + \frac{1}{2}\left(\sqrt{1 - \Delta_3^2(k)/\Delta_4^2(k)}\right)^{-1}. \tag{62}$$

Thus, we have identified relationship between the presented theory and the viscoelastic models. Although both the simple and extended viscoelastic models do not satisfy the high-order sum rules, these models can yield the correct results for the spectral features at the frequencies much smaller than $2\sqrt{\Delta_4^2(k)}$. Therefore, the extended viscoelastic model can be used as a sufficiently convenient approximation to study the relaxation process with the characteristic time scales larger than $1/(2\sqrt{\Delta_4^2(k)})$. This is directly evident from obtained above the simple analytical expansion for the TCF $M_2(k,\ t)$. Further, equations (60)–(62) set correspondence between the parameters of the viscoelastic models and the frequency parameters (the spectral moments of $S(k,\omega)$).

3.2. Hydrodynamic limit

Relation for the dynamic structure factor $S(k,\omega)$ at the hydrodynamic limit (see equation (1)) can be exactly rewritten as the ratio of the biquadratic polynomial to the bicubic polynomial:

$$2\pi\frac{S(k,\omega)}{S(k)} = \frac{a_1(k)\omega^4 + a_2(k)\omega^2 + a_3(k)}{\omega^6 + b_1(k)\omega^4 + b_2(k)\omega^2 + b_3(k)}, \tag{63a}$$

where the coefficients of the polynomials are defined as follows

$$a_1(k) = \frac{2}{\gamma}\left[(\gamma-1)D_T k^2 + \Gamma k^2\right], \tag{63b}$$

$$a_2(k) = \frac{2}{\gamma}\left\{2(\gamma-1)D_T k^2\left[(\Gamma k^2)^2 - (c_s k)^2\right] + (\Gamma k^2)\left[(\Gamma k^2)^2 + (c_s k)^2 + (D_T k^2)^2\right]\right\}, \tag{63c}$$

$$a_3(k) = \frac{2}{\gamma} D_T k^2\left[(\Gamma k^2)^2 + (c_s k)^2\right] \times \left\{(\gamma-1)\left[(\Gamma k^2)^2 + (c_s k)^2\right] + (D_T k^2)(\Gamma k^2)\right\}, \tag{63d}$$

$$b_1(k) = 2(\Gamma k^2)^2 - 2(c_s k)^2 + (D_T k^2)^2, \tag{63e}$$

$$b_2(k) = 2(D_T k^2)^2\left[(\Gamma k^2)^2 - (c_s k)^2\right] + \left[(\Gamma k^2)^2 + (c_s k)^2\right]^2, \tag{63f}$$

$$b_3(k) = (D_T k^2)^2\left[(\Gamma k^2)^2 + (c_s k)^2\right]^2. \tag{63g}$$

As seen from equation (63*a*), the coefficients in equation (63*a*) at the low-k limit have the following k-dependence: $a_1(k) \sim k^2$, $a_2(k) \sim k^4$, $a_3(k) \sim k^6$, $b_1(k) \sim k^2$, $b_2(k) \sim k^4$ and $b_3(k) \sim k^6$.

On the other hand, inserting expansion (54) into relation (42*a*) one obtains

$$2\pi\frac{S(k,\omega)}{S(k)} = \frac{\mathcal{B}_1(k)\omega^4 + \mathcal{B}_2(k)\omega^2 + \mathcal{B}_3(k)}{\omega^6 + \mathcal{A}_1(k)\omega^4 + \mathcal{A}_2(k)\omega^2 + \mathcal{A}_3(k)}, \tag{64a}$$

where

$$\mathcal{B}_1(k) = \frac{\Delta_1^2(k)\Delta_2^2(k)\Delta_3^2(k)}{16\Delta_4^2(k)\sqrt{\Delta_4^2(k)}(\Delta_4^2(k) - \Delta_3^2(k))}, \tag{64b}$$

$$\mathcal{B}_2(k) = \frac{\Delta_1^2(k)\Delta_2^2(k)\Delta_3^2(k)}{4\sqrt{\Delta_4^2(k)}(\Delta_3^2(k) - \Delta_4^2(k))}, \tag{64c}$$

$$\mathcal{B}_3(k) = \frac{2\Delta_1^2(k)\Delta_2^2(k)\Delta_3^2(k)\sqrt{\Delta_4^2(k)}}{\Delta_4^2(k) - \Delta_3^2(k)}, \tag{64d}$$

and the coefficients $\mathcal{A}_1(k)$, $\mathcal{A}_2(k)$ and $\mathcal{A}_3(k)$ are defined by equation (42*b*).

Thus, theoretical model (42*a*) for the dynamic structure factor can be reduced to the hydrodynamic result at long wavelengths and low frequencies.

3.3. Generalized hydrodynamics

The basic idea of the generalized hydrodynamics consists in introducing the k-dependent relaxation processes into the linearized hydrodynamics equations [14]. Then, the dynamic structure factor $S(k,\omega)$ will be modified, and it takes a more complicated form in comparison with hydrodynamic equation for $S(k,\omega)$, i.e. equation (1). As shown in [14, 58], the dispersion relation for this case can be written as follows

$$\omega(k) = c_s k = c_{s,0} k\sqrt{S + \sqrt{S^2 + \frac{1}{(c_{s,0}k\tau)^2}}}, \tag{65a}$$

$$S = \frac{1}{2}\left[\frac{c_{s,\infty}^2}{c_{s,0}^2} - \frac{1}{(c_{s,0}k\tau)^2}\right]. \tag{65b}$$

Here, $c_{s,0}$ is the low frequency speed of sound, $c_s = \omega/k$ is the speed of sound at the given frequency ω, $c_{s,\infty}$ is the high frequency sound velocity, and τ is the relaxation time[2].

As seen, dispersion relation (65*a*) is similar to dispersion law (43*b*) with only difference of the sign under the inner radicand. Note that the negative contribution under the inner radicand in equation (43*b*), i.e. $-3\mathcal{A}_2(k)$, provides an impact into the decreasing $\omega_s(k)$ at the wavenumbers from the range $k \in (k_m/2;\ k_m)$. Further, the quantity S in equation (65*a*) is identified with the coefficient $\mathcal{A}_1(k)$ in equation (43*b*):

$$S \to \mathcal{A}_1(k).$$

Note that the coefficient $\mathcal{A}_1(k)$ takes the negative values (see, for example, table 1 with values of this coefficient for liquid lithium).

3.4. High-k limit

The regime of the free-particle dynamics arises at the large wavenumbers, i.e. $k > k_m$, corresponding to wavelengths comparable with and smaller than the mean free path of a moving particle. Time- and spatial-scales are so short that there is, in fact, no any vibrational dynamics. The dynamic structure factor for the regime takes a sense of the self-dynamic structure factor $S_s(k,\omega)$ measurable in INS and characterizing a single-particle dynamics [12]. The static structure factor for this k-range approaches unity, i.e. $S(k) \to 1$ [5]. As a result, all the contributions in expressions for the frequency parameters, $\Delta_2^2(k)$, $\Delta_3^2(k)$ and etc, responsible for the particles interaction can be omitted. Then, taking into account equations (26*a*)–(26*c*) one obtains

$$\Delta_1^2(k) = (v_T k)^2,\ \Delta_2^2(k) = 2\Delta_1^2(k),\ \Delta_3^2(k) = 3\Delta_1^2(k),\ \ldots. \tag{66}$$

Substituting the frequency parameters into fraction (30) one has

$$\widetilde{F}(k,s) = \cfrac{1}{s + \cfrac{\Delta_1^2(k)}{s + \cfrac{2\Delta_1^2(k)}{s + \cfrac{3\Delta_1^2(k)}{s + \ddots}}}}. \tag{67}$$

[2] Do not confuse the quantity S in equation (65*a*) with the static structure factor $S(k)$.

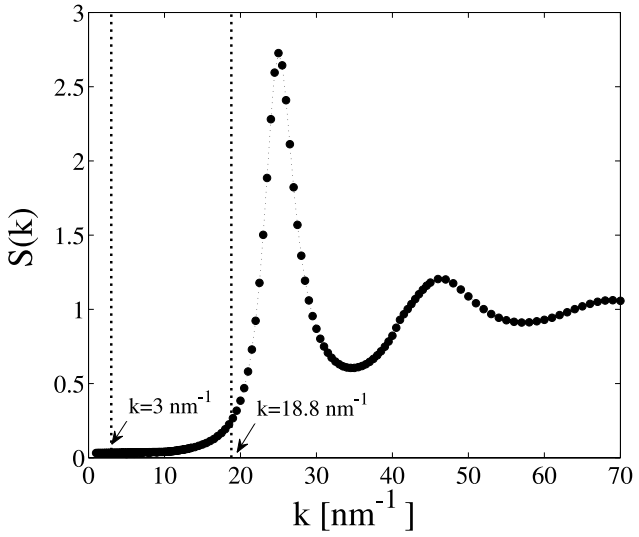

Figure 1. Static structure factor of liquid lithium at the temperature $T = 463$ K measured by x-ray diffraction; data taken from [63]. Two vertical dotted lines mark out the wavenumber range considered in this study. The main peak of the static structure factor $S(k)$ is located at $k_m \simeq 24.4$ nm $^{-1}$.

This is continued fraction representation of the Laplace transform of the Gaussian function

$$F(k,t) = \exp\left(-\frac{(v_T k)^2 t^2}{2}\right). \tag{68}$$

Then, taking into account equation (17), one obtains the correct result for the dynamic structure factor at the high-k limit:

$$S(k,\omega) = \sqrt{\frac{1}{2\pi}}\frac{1}{v_T k}\exp\left(-\frac{\omega^2}{2(v_T k)^2}\right), \tag{69}$$

which was mentioned in section 1.

We see that expression (69) is the rigorous theoretical result obtained in a self-consistent manner from the exact relation (66) for the frequency parameters. Therefore, relation (42*a*) for the dynamic structure factor transforms into relation (69), when condition (34) for the frequency parameters changes to (66).

4. Dynamic structure factor of liquid lithium near melting

The first studies of the microscopic collective ion dynamics of liquid lithium by means of inelastic scattering methods were performed by De Jong and Verkerk [55], and Burkel and Sinn [56]. Then, IXS studies of this liquid metal were carried out by Scopigno *et al* for the more extended range of the wavenumbers.

The features of the density fluctuations dynamics in a liquid depend on a spatial scale, where these fluctuations emerge. Therefore, it is convenient to measure the spatial scale in terms of the location of the first peak k_m in the static structure factor $S(k)$. In the given study, the equilibrium density fluctuations dynamics in liquid lithium at the temperature $T = 475$ K is considered. For liquid lithium at this temperature, the quantity k_m equals to $\simeq 24.4\,\mathrm{nm}^{-1}$ (see figure 1). Thus, the extended wavenumber range $k \in [3.0;\ 18.8]\ \mathrm{nm}^{-1}$ is covered by our study. According to the classification given in [10] (see pp 927–30), the wavenumber $k = 3.0\,\mathrm{nm}^{-1}$ corresponds to $k/k_m = 0.12$ and defines the lower boundary of a hypothetical isothermal dynamical region, whereas the wavenumber $k = 18.8\,\mathrm{nm}^{-1}$ is identical to $k/k_m = 0.77$ and is associated with the upper boundary of the so-called generalized hydrodynamic region [10]. Although the theory presented in section 2.2 should be also valid for longer wavelengths, $k = 3.0\,\mathrm{nm}^{-1}$ is the smallest wavenumber with available IXS data for liquid lithium [38]. On the other hand, the wavenumber $k = 18.8\,\mathrm{nm}^{-1}$ corresponds to the shortest wavelengths at which the collective acoustic-like dynamics is still supported in this liquid and expression (42*a*) for the dynamic structure factor $S(k,\omega)$ is valid.

To compare the theoretical classical dynamic structure factor $S(k,\omega)$ with the scattering intensity $I(k,\omega)$, one needs to account for the quantum effects by means of the detailed balance condition

$$S_q(k,\omega) = \frac{\hbar\omega/k_\mathrm{B}T}{1-\exp(-\hbar\omega/k_\mathrm{B}T)}S(k,\omega), \tag{70a}$$

where $S_q(k,\omega)$ is the quantum-mechanical structure factor. Then, the experimental resolution effects must be included into consideration through the convolution

$$I(k,\omega) = E(k)\int R(k,\omega-\omega')S_q(k,\omega')\mathrm{d}\omega', \tag{70b}$$

where $E(k)$ and $R(k,\omega)$ are the characteristics of the IXS experiment. The quantity $E(k)$ depends on analyzer efficiency and on the atomic form factor [10], whereas $R(k,\omega)$ is the experimental resolution function. The dynamic structure factor $S(k,\omega)$ and the scattering intensity $I(k,\omega)$ of liquid lithium at $T = 475$ K were defined by means of equations (42*a*) and (70*a*), (70*b*) at the wavenumbers $k = 3.0$, 7.0, 11.2, 12.0 and $18.8\,\mathrm{nm}^{-1}$. To determine $S(k,\omega)$ by means of relation (42*a*) we first need to compute the four frequency parameters $\Delta_1^2(k)$, $\Delta_2^2(k)$, $\Delta_3^2(k)$ and $\Delta_4^2(k)$. This can be done by two independent methods.

Let us consider the *first method* used by us to determine these parameters for the case of liquid lithium at the considered thermodynamic state. The frequency parameter $\Delta_1^2(k)$ has been computed exactly by means of equation (26*a*) (the first equality in this equation) with the experimental values of the static structure factor $S(k)$ from [63]. The values of the parameter $\Delta_2^2(k)$ were determined from the first equality of equation (26*b*) with the pseudopotential $u(\mathbf{r})$ proposed by Gonzalez *et al* [35] and with the radial distribution function $g(r)$ computed on the basis of this potential. It is important to note that the theoretical radial distribution function is consistent with the x-ray diffraction data [63]. Further, although the frequency parameters $\Delta_3^2(k)$ and $\Delta_4^2(k)$ can be also computed theoretically through the integral expressions with the three- and four-particle distribution functions (see, for example, equation (26*c*)), this is difficult to implement. Therefore, one can take these two parameters as the fitting parameters. The

Table 1. Values of the frequency parameters $\Delta_1^2(k)$, $\Delta_2^2(k)$, $\Delta_3^2(k)$, $\Delta_4^2(k)$ (in units of $\times 10^{24}$ s^{-2}) and values of the coefficients $\mathcal{A}_1(k)$ ($\times 10^{26}$ s^{-2}), $\mathcal{A}_2(k)$ ($\times 10^{52}$ s^{-4}), $\mathcal{A}_3(k)$ ($\times 10^{78}$ s^{-6}) of the polynomial in relation (42*a*) for the dynamic structure factor $S(k,\omega)$.

k (nm^{-1})	$\Delta_1^2(k)$	$\Delta_2^2(k)$	$\Delta_3^2(k)$	$\Delta_4^2(k)$	$\mathcal{A}_1(k)$	$\mathcal{A}_2(k)$	$\mathcal{A}_3(k)$
3.0	183 ± 10	210 ± 30	1500 ± 230	$17\,731 \pm 4500$	-6.61	11.0	4.5
7.0	845 ± 30	1109 ± 150	7110 ± 1350	$87\,905 \pm 23\,500$	-33.78	294.8	446.2
11.2	1346 ± 50	1500 ± 220	$10\,000 \pm 3100$	$179\,700 \pm 43000$	-52.07	681.0	1071.8
12.0	1545 ± 80	1609 ± 240	$12\,000 \pm 3000$	$157\,600 \pm 40\,500$	-54.48	729.8	2369.9
18.8	971 ± 60	1589 ± 210	$11\,100 \pm 2300$	$68\,540 \pm 20\,000$	-32.77	316.4	2027.0

first way is to calculate the frequency moments $\omega^{(6)}(k)$ and $\omega^{(8)}(k)$ for the *experimental* spectra of the dynamic structure factor $S(k,\omega)$ (see equation (18)), and then to find the values of $\Delta_3^2(k)$ and $\Delta_4^2(k)$ by means of sum rules (25*c*) and (25*d*)[3]. We have evaluated these parameters, $\Delta_3^2(k)$ and $\Delta_4^2(k)$, by a different way. Namely, if one associates the parameter $\Delta_4^2(k)$ with the correct (experimental) value of $S_{\rm exp}(k,\omega)$ at $\omega = 0$ in accordance with relation (42*a*), i.e.

$$\Delta_4^2(k) = \left[\frac{\pi S_{\rm exp}(k,\omega=0)}{S(k)}\,\frac{\Delta_1^2(k)\Delta_3^2(k)}{\Delta_2^2(k)}\right]^2, \qquad (71)$$

then the quantity $\Delta_3^2(k)$ must be taken directly as fitting parameter. Thus, the two parameters, $\Delta_3^2(k)$ and $\Delta_4^2(k)$, are used as adjustable in such the realization of the theoretical model (42*a*) for $S(k,\omega)$. To our knowledge, there is no other theory for the dynamic structure factor of liquids (even of simple liquids), which operates without fitting parameters, or applies one or two fitting parameters only and yields, herewith, satisfactory agreement with experimental IXS/INS data for the wavenumber range. Further, we recall that the frequency parameters are not the special model parameters, but are the quantities, that determine the sum-rules of the scattering law. Consequently, if the theoretical scheme is capable to reproduce all the features of the scattering law and the scheme satisfies the sum-rules, then theoretical and experimental values of the frequency parameters must be comparable or identical.

The first six frequency parameters, $\Delta_1^2(k)$, $\Delta_2^2(k)$, $\Delta_3^2(k)$, $\Delta_4^2(k)$, $\Delta_5^2(k)$ and $\Delta_6^2(k)$, were also evaluated by means of the *second method*. In accordance with this method, the configuration data obtained from the simulations with the given interparticle potential $u(\mathbf{r})$ is required only. Then, the frequency moments $\omega^{(2j)}(k)$ and the frequency parameters $\Delta_j^2(k)$ with $j = 1, 2, 3, \ldots$, can be determined by means of the original definitions: equation (10) with relations (5) and (9). The computational details are given in appendix. This method yields results for the low-order frequency moments and parameters with high accuracy, that is confirmed by agreement of the results with the

[3] According to the method, these moments are evaluated for the dynamic structure factor, which has to be extracted by deconvolution of the experimental scattering intensity and the experimental resolution function. For the case of liquid metals, the dynamic structure factor at finite wavenumbers decays (in frequency) to zero over 100 THz range. Therefore, all the moments have to be finite and definable by this method. Computational problems can be here only due to deconvolution procedure. Nevertheless, one needs to note that the resolution function is well approximated by the Dirac delta-function for the case of INS data. Therefore, the scattering intensity is proportional to the dynamic scattering function, and the method for evaluating the spectral moments is expected to be efficient.

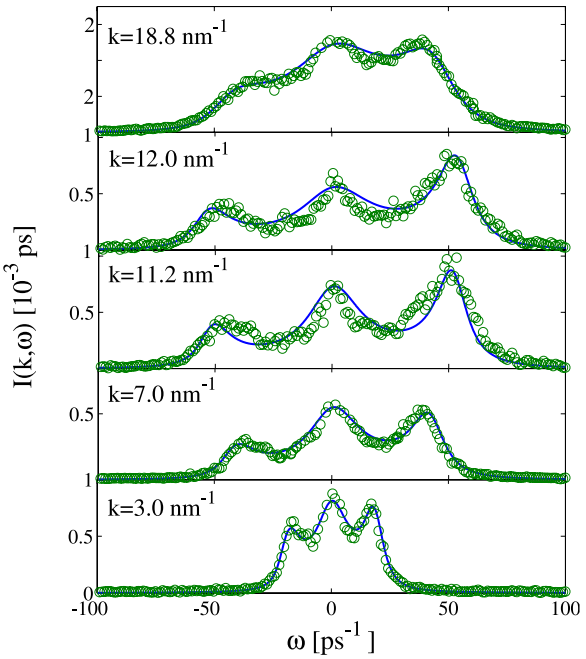

Figure 2. Scattering intensity $I(k,\omega)$ of liquid lithium at the temperature $T = 475$ K and several values of the wavenumber $k < k_m$, where $k_m = 24.4\,\text{nm}^{-1}$ corresponds to the first peak position of the static structure factor $S(k)$. Open circles ($\circ$) represent experimental IXS data [10], full lines ($-$) depict the theoretical dynamical structure factor $S(k,\omega)$ (see equation (42*a*)) modified to takes into account the quantum-mechanical detailed balance condition and the experimental resolution effects.

data for the experimental static structure factor $S(k)$ and with the exact theoretical values for $\Delta_1^2(k)$ and $\Delta_2^2(k)$ evaluated from equations (26*a*) and (26*b*), respectively. Because of the numerical differentiation procedure used in this method, the magnitude of the statistical error of an evaluated frequency parameter $\Delta_j^2(k)$ increases with increasing order j, where $j = 3, 4, 5, \ldots$. Nevertheless, we find that the values of $\Delta_3^2(k)$ and $\Delta_4^2(k)$ agree within the confidence interval with the results obtained from the fitting procedure in accordance with the first method. This confirms that the values of the frequency parameters $\Delta_1^2(k)$, $\Delta_2^2(k)$, $\Delta_3^2(k)$ and $\Delta_4^2(k)$ obtained by the first method can be adopted; the numerical values of these parameters are given in table 1. The results for the frequency parameters from both the methods will be presented in figure 5.

In figure 2, the theoretical scattering intensity $I(k,\omega)$ is compared with the experimental IXS data [10]. As seen, the presented theory with expression (42*a*) for the dynamic structure factor has excellent agreement with experimental data. The theoretical intensity $I(k,\omega)$ accounts for the spectral

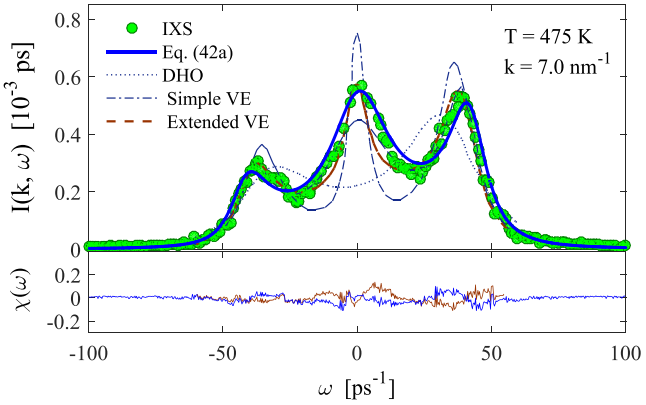

Figure 3. Top: scattering intensity of liquid lithium at $T = 475\,\mathrm{K}$ and $k = 7.0\,\mathrm{nm}^{-1}$: IXS data (full circles) and results for the DHO model (dotted line), the simple viscoelastic model (−·−), the extended viscoelastic model (dashed line) and the results of the theoretical model (42*a*). IXS data and results for DHO, simple and extended viscoelastic models are taken from [38]. Bottom: difference between the experimental data and the theoretical values, $\chi(\omega) = I_{\mathrm{IXS}}(k,\omega) - I_{\mathrm{th}}(k,\omega)$, computed for the extended viscoelastic model and for the theoretical model (42*a*).

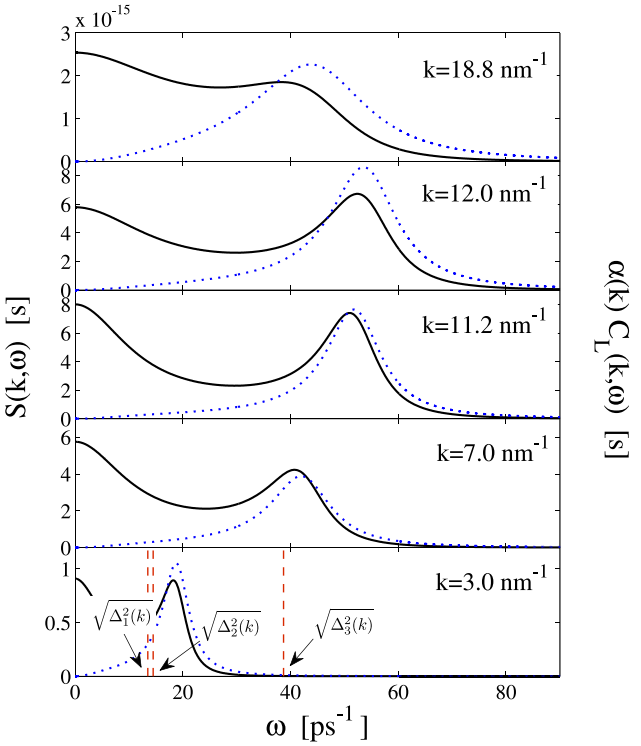

Figure 4. Dynamic structure factor $S(k,\omega)$ (solid line) and scaled longitudinal current correlation function $\alpha(k)C_L(k,\omega)$ (dotted line) of liquid lithium at the same temperature and fixed wavenumbers as in figure 2. The dimensionless coefficient $\alpha(k)$ takes the values $5\cdot10^{-5}$, $5\cdot10^{-5}$, $15\cdot10^{-5}$, $2\cdot10^{-4}$, and $3\cdot10^{-3}$ at $k = 3.0$, 7.0, 11.2, 12.0 and $18.8\,\mathrm{nm}^{-1}$, respectively. Red vertical dashed lines for the bottom plot correspond to the frequencies $\sqrt{\Delta_1^2(k)}$, $\sqrt{\Delta_2^2(k)}$ and $\sqrt{\Delta_3^2(k)}$ at $k = 3.0\,\mathrm{nm}^{-1}$.

features. The values of the coefficients $\mathcal{A}_1(k)$, $\mathcal{A}_2(k)$ and $\mathcal{A}_3(k)$ are given in table 1.

We note that efficiency of some theoretical models to analyze the same IXS data was verified previously by Scopigno

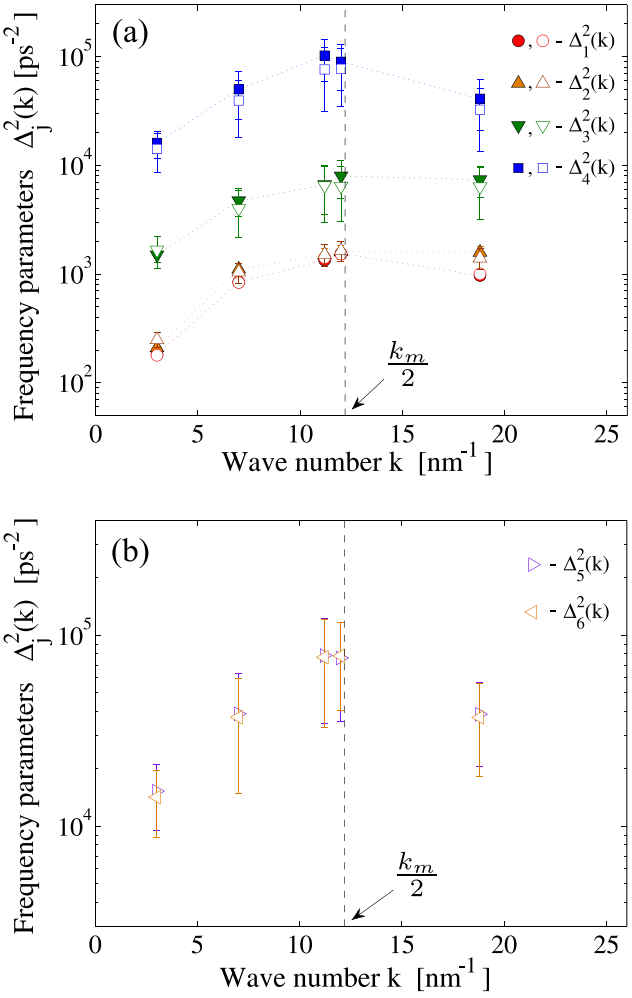

Figure 5. Wavenumber dependence of the frequency parameters $\Delta_1^2(k)$, $\Delta_2^2(k)$, $\Delta_3^2(k)$, $\Delta_4^2(k)$, $\Delta_5^2(k)$ and $\Delta_6^2(k)$ in logarithmic scale. Dashed vertical line corresponds to the wavenumber $k = k_m/2 \simeq 12.2$ nm $^{-1}$. Full markers correspond to the theoretical values evaluated by the first way (see the text before equation (71)), whereas transparent markers indicate the values estimated theoretically by the second way—on the basis of equations (9) and (10) with the configuration data (for details, see appendix).

et al in [38]. Comparison of experimental data and theoretical results was carried out for the specific spectrum at $k = 7.0\,\mathrm{nm}^{-1}$. As was clearly demonstrated (figure 5 in [38]), both the damped harmonic oscillator model and the simple viscoelastic model cannot reproduce the lineshape of the scattering intensity. The agreement with the experimental data appears only for the extended viscoelastic model, where the time dependence of the TCF $M_2(k, t)$ is approximated by the linear combination of the three exponential decay laws associated with thermal and viscous fluctuations. In figure 3, we reproduce all the data from figure 5 of [38] supplemented by our theoretical results. Although the extended viscoelastic model of [38] and our model with equation (42*a*) do not yield the identical lineshapes of $I(k,\omega)$, both the models are characterized by a comparable agreement with the experimental data. Further, as it was demonstrated in section 3, our theory does not contradict to the extended viscoelastic model and can provide justification for the expansion of the TCF $M_2(k, t)$

over exponential functions. For the case of liquid lithium with the estimated frequency parameters $\Delta_3^2(k)$ and $\Delta_4^2(k)$ at the considered wavenumbers, we find from equation (61) that the first relaxation time $\tau_\alpha(k)$ takes the values from the range [0.1;1] ps, whereas the second relaxation process with $\tau_\mu(k)$ occurs over time scales ∼0.01 ps. These estimates are in agreement with results obtained in [38, 57] with the extended viscoelastic model.

In figure 4, the classical dynamic structure factor $S(k,\omega)$ and the longitudinal current correlation function $C_L(k,\omega)$ computed on the basis of relations (42*a*) and (22) are shown. These results are presented for the same wavenumbers as for the scattering intensity $I(k,\omega)$ in figure 2. To make clear correspondence between $S(k,\omega)$ and $C_L(k,\omega)$, the spectra of $C_L(k,\omega)$ are scaled onto the coefficient $\alpha(k)$. As seen, the high-frequency peak of $S(k,\omega)$ and the peak of $C_L(k,\omega)$ are very close, and both the dispersion curves $\omega_{\max}(k)$ and $\omega_c(k)$ have to be practically identical for the considered wavenumber range [64]. Further, there is no gap between the central component $S(k,\omega=0)$ and the high-frequency component $S(k,\omega_{\max})$ as it usually have to be for $S(k,\omega)$ in the hydrodynamic limit (at $k\to 0$) [12]. So, the lineshape of the dynamic structure factor $S(k,\omega)$ at the finite k represents the result of complicated mixing of relaxing and propagative modes. Hence, simple separation of the density fluctuations into two types associated with mechanical processes and with thermal processes is not possible.

The frequency parameters evaluated by means of the two methods are shown in figure 5. The wavenumber dependence of these parameters, $\Delta_1^2(k)$, $\Delta_2^2(k)$, $\Delta_3^2(k)$ and $\Delta_4^2(k)$, are smooth and similar. The parameters increase with increasing wavenumber and saturate at $k\simeq k/k_m = 12.2\,\mathrm{nm}^{-1}$. Then, the frequency parameters start to decrease with further increase of the wavenumber k. In fact, the k-dependence of the frequency parameters is similar to the dispersion curve $\omega_{\max}(k)$ of the acoustic-like excitations in simple liquid [11] (compare with figure 6 (top)). Further, although the parameters $\Delta_1^2(k)$ and $\Delta_2^2(k)$ take very close values, nevertheless, the correspondence $\Delta_{j+1}^2(k)\geqslant\Delta_j^2(k)$ for the frequency parameters $\Delta_j^2(k)$, $j=1,\,2,\,3,\,4$, still occurs at the considered wavenumbers. The first three frequency parameters take the values corresponding to the square *THz* frequency scale (or to the inverse square *ps* timescale). Therefore, these correspond to the typical frequencies of local density fluctuations in a liquid at microscopic spatial scales. The frequency parameter $\Delta_4^2(k)$ takes the largest values in comparison with $\Delta_1^2(k)$, $\Delta_2^2(k)$ and $\Delta_3^2(k)$. In fact, the parameter $\Delta_4^2(k)$ defines the upper limit of the frequency domain associated with the density fluctuations. For example, let us consider the dynamic structure factor $S(k,\omega)$ at $k=3.0\,\mathrm{nm}^{-1}$ (see the bottom inset in figure 4). Here, the scattering function is completely damped at the frequencies $\omega\geqslant 30$ ps^{-1}. The first three frequency parameters are $\Delta_1^2=183\,\mathrm{ps}^{-2}$, $\Delta_2^2=210\ \mathrm{ps}^{-2}$ and $\Delta_3^2=1500\ \mathrm{ps}^{-2}$, whereas the parameter $\Delta_4^2=177\cdot 10^2\ \mathrm{ps}^{-2}$ is much larger than $\omega^2=900\ \mathrm{ps}^{-2}$. One can see from figure 5 that both the conditions, $\Delta_4^2(k)\gg\omega^2$ (see also inequality (33)) and $\Delta_4^2(k)\approx\Delta_5^2(k)\approx\Delta_6^2(k)$ (relation (34)) are completely supported by obtained values of

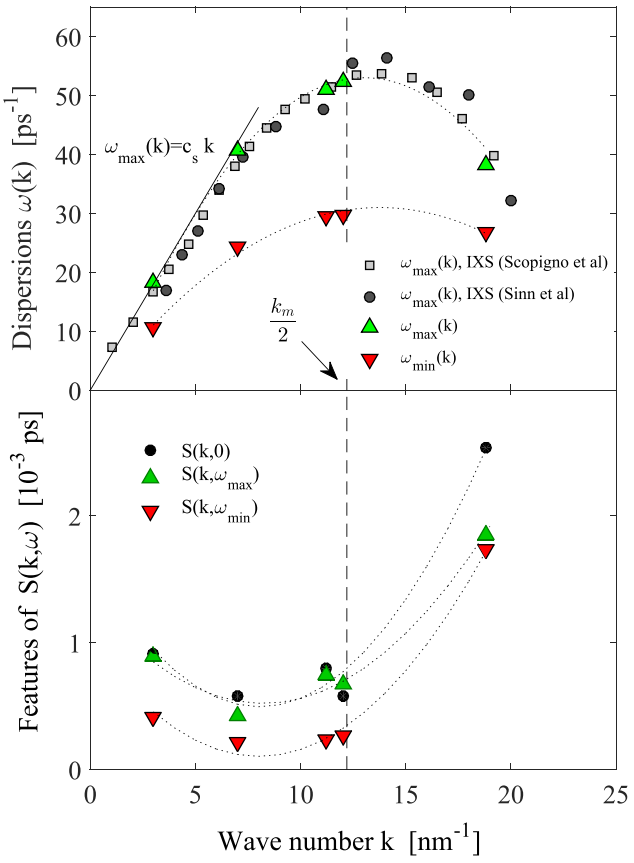

Figure 6. Top: sound dispersion $\omega_{\max}(k)$ and wavenumber-dependent frequency $\omega_{\min}(k)$ evaluated from equations (43*b*) and (43*c*); sound dispersions from IXS data of Scopigno *et al* [38] (full squares) and Sinn *et al* [16] (full circles). Solid line at low wavenumbers corresponds to hydrodynamic frequency of the Mandelshtam–Brillouin doublet $\omega_c(k)=c_sk$ with the adiabatic sound velocity $c_s\simeq 6000$ m s^{-1}. Bottom: wavenumber dependent spectral features: zeroth-frequency spectral component $S(k,\omega=0)$, high-frequency component $S(k,\omega_{\max})$, scattering intensity at the minimum $S(k,\omega_{\min})$. Dashed vertical line corresponds to the border of the first pseudo-Brillouin zone.

the frequency parameters. Moreover, there is the following regularity between the frequencies $\sqrt{\Delta_1^2(k)}$, $\sqrt{\Delta_2^2(k)}$ and the spectral features of the dynamic structure factor $S(k,\omega)$: both the frequencies $\sqrt{\Delta_1^2(k)}$ and $\sqrt{\Delta_2^2(k)}$ are located between the minimum and the high-frequency maximum of $S(k,\omega)$, i.e. within the frequency range $[\omega_{\min}(k);\ \omega_{\max}(k)]$.

By means of equations (46)–(48), one can determine the hydrodynamic parameters from the wavenumber dependence of the frequency parameters in the low-k range. We obtain that the sound velocity of liquid lithium at the temperature $T=475\,\mathrm{K}$ is $c_s\simeq 6000\pm 1200$ m s^{-1}, which is larger than the value 4550 m s^{-1} given in [15] for liquid lithium at the melting temperature T_m. Further, our estimates for the thermal diffusivity yield $D_T\simeq 21.5\pm 3.5$ nm^2 ps^{-1}. This value is comparable with 19.1 nm^2 ps^{-1} given for D_T of liquid lithium in [65]. Finally, we find that the sound attenuation coefficient Γ takes the value $\simeq 18.4\pm 3.5\,\mathrm{nm}^2\,\mathrm{ps}^{-1}$.

Since relation (42*a*) reproduces the lineshape of the dynamic structure factor $S(k,\omega)$, then all the spectral features can be also recovered. In figure 6(top), the frequencies $\omega_{\max}(k)$ and $\omega_{\min}(k)$ associated with locations of the high-frequency maximum and minimum of $S(k,\omega)$ are presented as functions of the wavenumber k. It is necessary to note that the dispersion curve $\omega_{\max}(k)$ in the low-k limit must be extrapolated into the hydrodynamic result $\lim_{k\to 0}\omega_{\max}(k) = c_s k$, whereas $\omega_{\min}(k)$ in the low-k asymptotics must be characterized by a gap, which appears because of the separation of the Rayleigh and Brillouin components. It is seen in figure 6(bottom) that the evaluated components $S(k,\omega=0)$, $S(k,\omega_{\max})$ and $S(k,\omega_{\min})$ as functions of the wavenumber are correlated. Namely, the intensities $S(k,0)$ and $S(k,\omega_{\min})$ have similar $k-$dependence. Further, the Rayleigh component $S(k,0)$ and the Brillouin component $S(k,\omega_{\max})$ take practically the same values for the wavenumbers $k \leqslant k_m/2$ and yield the ratio $S(k,0)/S(k,\omega_{\max}) \simeq 1$.

5. Concluding remarks

In a liquid, the overall wavenumber range available for inelastic scattering experiments with photons, neutrons and/or x-rays includes three ranges: the hydrodynamic range (limit), the broad meso-microscopic range and the free-particle dynamics range (limit). An extension of the hydrodynamic theory is possible up to such finite wavenumbers, where the hydrodynamic quantities—the viscosity, the thermal conductivity, the sound absorption and others—still have a physical meaning. Let us consider the extended wavenumber range, which includes the wavenumbers corresponding to the hydrodynamic limit and the wavenumbers associated with mesoscopic–microscopic scales. According to the ideas of the generalized hydrodynamics, the viscosity must be transformed into a k-dependent parameter when we consider the wavenumbers corresponding to the mesoscopic range. Consequently, at microscopic scales comparable with the size of the second or third pseudo-coordination shells, this macroscopical parameter (the viscosity) must be transformed into a characteristic that takes into account the cumulative result of interparticle interactions within the range. On the other hand, the wavenumber k decreases from large values associated with the limit of a free moving particle to lower values corresponding to mesoscopic sizes. Here, with decreasing wavenumber, such a characteristic as the thermal velocity of a free moving particle is converted to the phase velocity of the particles enclosed in appropriate spatial range $\ell \sim 2\pi/k$. Therefore, the theoretical methodology relevant to describe the mesoscopic–microscopic dynamics in liquids has to employ such the quantities as the particle distributions, the interaction energy between the particles and the frequency characteristics of vibration dynamics of a particle with respect to its neighbors (similar to the Einstein frequency).

The theoretical scheme presented in this study exploits the spectral moments of the dynamic structure factor $S(k,\omega)$ and does not apply the assumptions about how many relaxing and propagating modes have to be taken into account. It is important that the spectral moments are determined by the interparticle potential and the structural characteristics. On the other hand, the spectral moments define the sum rules and cannot be considered as arbitrary model parameters. That is important, the presented theoretical scheme satisfies all the sum rules of the scattering law. Moreover, the theoretical relation obtained for the dynamic structure factor $S(k,\omega)$ transforms approximatively at the certain conditions associated with convergence of the high-order frequency parameters to well known hydrodynamic result for $S(k,\omega)$; as well as the theory yields the correct scenario for the high-k limit.

The dynamic structure factor is the characteristic of the longitudinal collective dynamics in liquids [12]. The scattering spectra can also contain marks of the transverse collective excitations with the frequencies lower than $\omega_c(k) = c_s k$ [66]. However, for the case of an equilibrium simple liquid, the intensity of these excitations is very small and it is barely noticeable in the scattering spectra. In particular, this is evidenced by results of figure 2 in [67], where representation of the scattering spectra in terms of the corresponding longitudinal and transverse components for liquid Fe, Cu and Zn is given. Thus, it is reasonable to overlook the secondary transverse excitations in the analysis of the longitudinal dynamics. Further, according to the theoretical scheme presented in this study, the spectral density of any dynamical variable relevant to the structural relaxation in a liquid can be expressed in terms of its spectral (frequency) moments. Therefore, the presented theory can be directly extended to the case of the transverse collective dynamics.

Alignment of the high-order frequency parameters does not contradict to outcomes the linearized hydrodynamics. In fact, the alignment is identical to the assumption about equality of the TCFs $M_3(k,t)$ and $M_4(k,t)$. This allows one to define self-consistently the intermediate scattering function $F(k,t)$ and all other TCFs: $M_1(k,t)$, $M_2(k,t)$ and $M_3(k,t)$. In such a view, the presented theoretical scheme is similar in its construction to the mode-coupling theories adapted for ergodic systems [44], where the memory function $M_2(k,t)$ is expressed in terms of the intermediate scattering function $F(k,t)$. It should be noted that Reichman and Charbonneau (in [68] (discussion on p 21)) pointed to a possible extension of the mode-coupling theory, involving the shift of the 'mode-coupling closure' to the high-order memory function $M_4(k,t)$. This is directly corresponds to the theoretical scheme presented in this study.

In this study, we applied the theoretical approach to determine the dynamic structure factor and the scattering intensity at some selected wavenumbers for the case of liquid lithium. We chose this system to test our theory for the following reasons. As asserted in [33], the collective microscopic dynamics of this liquid can be more complicated than the dynamics of other liquid metals. Therefore, a microscopic theory may be experiencing difficulties in its application to liquid lithium. On the other hand, high quality experimental data are available for the microscopic structure and collective dynamics of liquid lithium [16, 36, 38]. We found that the theory is capable of reproducing all the features of the scattering intensity in agreement with IXS data. Finally, the presented theory utilizes the particle interaction potential and structural characteristics as input parameters. Therefore, this theory can be applied directly to the case of any simple fluid.

Acknowledgments

We thank T Scopigno for providing us with experimental IXS data and AG Novikov, VV Brazhkin and VN Ryzhov for useful discussions. We also grateful to LE González for his advice on the lithium pseudopotential and to RM Khusnutdinoff for his help with molecular dynamics simulations. The reported study was supported in part by RFBR according to the research project No. 18-02-00407. The authors are thankful to the Ministry of Education and Science of the Russia Federation for supporting the research in the framework of the state assignment (3.2166.2017/4.6).

Appendix. The frequency parameters from configuration data. Details of molecular dynamics simulations

The wavenumber-dependent frequency parameters $\Delta_1^2(k)$, $\Delta_2^2(k)$, $\Delta_3^2(k)$, …, can be calculated on the basis of configuration data of the considered many-particle system. These data must include the coordinates, velocities and accelerations, i.e. $\{\mathbf{r}_1,\ \mathbf{v}_1,\ \mathbf{a}_1;\ \mathbf{r}_2,\ \mathbf{v}_2,\ \mathbf{a}_2;\ \ldots;\ \mathbf{r}_N,\ \mathbf{v}_N,\ \mathbf{a}_N\}$, of all the N particles forming the system, that is usually available, for example, from molecular dynamics simulations with the given interparticle potential. Then, the dynamical variables $A_0(k)$, $A_1(k)$, $A_2(k)$ etc can be computed on the basis of equation (5) and recurrent relation (9), whereas the frequency parameters can be computed from equation (10).

In particular, we find for the first five dynamical variables the following exact expressions:

$$A_0(k,t) \equiv \rho_k(t) = \frac{1}{\sqrt{N}}\sum_{n=1}^{N}\left[\cos(\mathbf{k}\cdot\mathbf{r}_n(t)) + \mathrm{i}\sin(\mathbf{k}\cdot\mathbf{r}_n(t))\right], \tag{A.1}$$

$$A_1(k,t) = \frac{1}{\sqrt{N}}\sum_{n=1}^{N}\left[\left(\mathbf{k}\cdot\mathbf{v}_n(t)\right)\left\{-\sin(\mathbf{k}\cdot\mathbf{r}_n(t)) + \mathrm{i}\cos(\mathbf{k}\cdot\mathbf{r}_n(t))\right\}\right], \tag{A.2}$$

$$\begin{aligned}A_2(k,t) = \frac{1}{\sqrt{N}}\sum_{n=1}^{N}\Bigg[&\left(\mathbf{k}\cdot\mathbf{a}_n(t)\right)\left\{-\sin(\mathbf{k}\cdot\mathbf{r}_n(t)) + \mathrm{i}\cos(\mathbf{k}\cdot\mathbf{r}_n(t))\right\}\\ &+\left(\mathbf{k}\cdot\mathbf{v}_n(t)\right)^2\left\{-\cos(\mathbf{k}\cdot\mathbf{r}_n(t)) - \mathrm{i}\sin(\mathbf{k}\cdot\mathbf{r}_n(t))\right\}\Bigg]\\ &+\Delta_1^2(k)A_0(k,t),\end{aligned} \tag{A.3}$$

$$\begin{aligned}A_3(k,t) = \frac{1}{\sqrt{N}}\sum_{n=1}^{N}\Bigg[&\left(\mathbf{k}\cdot\frac{\mathrm{d}\mathbf{a}_n(t)}{\mathrm{d}t}\right)\left\{-\sin(\mathbf{k}\cdot\mathbf{r}_n(t)) + \mathrm{i}\cos(\mathbf{k}\cdot\mathbf{r}_n(t))\right\}\\ &+\left(\mathbf{k}\cdot\mathbf{v}_n(t)\right)^3\left\{\sin(\mathbf{k}\cdot\mathbf{r}_n(t)) - \mathrm{i}\cos(\mathbf{k}\cdot\mathbf{r}_n(t))\right\}\\ &+3\left(\mathbf{k}\cdot\mathbf{v}_n(t)\right)\left(\mathbf{k}\cdot\mathbf{a}_n(t)\right)\left\{-\cos(\mathbf{k}\cdot\mathbf{r}_n(t)) - \mathrm{i}\sin(\mathbf{k}\cdot\mathbf{r}_n(t))\right\}\Bigg]\\ &+\left[\Delta_1^2(k) + \Delta_2^2(k)\right]A_1(k,t)\end{aligned} \tag{A.4}$$

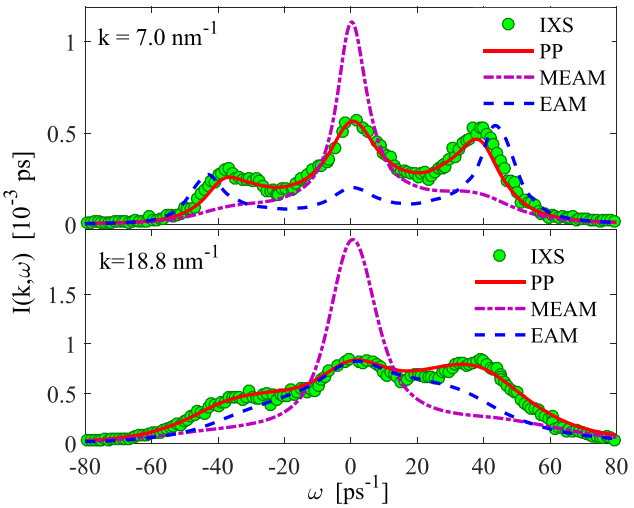

Figure A1. Scattering intensity of liquid lithium at the temperature $T = 475$ K and at the selected wavenumbers. Comparison experimental IXS data [38] and results of MD simulations with the model pseudopotential [35], with the EAM potential [69] and with the MEAM potential [70].

and

$$\begin{aligned}A_4(k,t) = \frac{1}{\sqrt{N}}\sum_{n=1}^{N}\Bigg[&\left(\mathbf{k}\cdot\frac{\mathrm{d}^2\mathbf{a}_n(t)}{\mathrm{d}t^2}\right)\left\{-\sin(\mathbf{k}\cdot\mathbf{r}_n(t)) + \mathrm{i}\cos(\mathbf{k}\cdot\mathbf{r}_n(t))\right\}\\ &+4\left(\mathbf{k}\cdot\mathbf{v}_n(t)\right)\left(\mathbf{k}\cdot\frac{\mathrm{d}\mathbf{a}_n(t)}{\mathrm{d}t}\right)\left\{-\cos(\mathbf{k}\cdot\mathbf{r}_n(t)) - \mathrm{i}\sin(\mathbf{k}\cdot\mathbf{r}_n(t))\right\}\\ &+3\left(\mathbf{k}\cdot\mathbf{a}_n(t)\right)^2\left\{-\cos(\mathbf{k}\cdot\mathbf{r}_n(t)) - \mathrm{i}\sin(\mathbf{k}\cdot\mathbf{r}_n(t))\right\}\\ &+6\left(\mathbf{k}\cdot\mathbf{v}_n(t)\right)^2\left(\mathbf{k}\cdot\mathbf{a}_n(t)\right)\left\{\sin(\mathbf{k}\cdot\mathbf{r}_n(t)) - \mathrm{i}\cos(\mathbf{k}\cdot\mathbf{r}_n(t))\right\}\\ &+\left(\mathbf{k}\cdot\mathbf{v}_n(t)\right)^4\left\{\cos(\mathbf{k}\cdot\mathbf{r}_n(t)) + \mathrm{i}\sin(\mathbf{k}\cdot\mathbf{r}_n(t))\right\}\Bigg]\\ &+\left(\Delta_1^2(k) + \Delta_2^2(k) + \Delta_3^2(k)\right)\left(A_2(k,t) - \Delta_1^2(k)A_0(k,t)\right)\\ &+\Delta_1^2(k)\Delta_3^2(k)A_0(k,t).\end{aligned} \tag{A.5}$$

The time derivatives $\mathrm{d}\mathbf{a}_n(t)/\mathrm{d}t$ and $\mathrm{d}^2\mathbf{a}_n(t)/\mathrm{d}t^2$ in equations (A.4) and (A.5) can be determined numerically by the finite difference method. Namely, one can apply the next simple scheme:

$$\frac{\mathrm{d}\mathbf{a}_n(t_{i+1})}{\mathrm{d}t} = \lim_{\Delta t\to 0}\frac{\mathbf{a}_n(t_{i+1}) - \mathbf{a}_n(t_i)}{\Delta t}, \tag{A.6}$$

$$\frac{\mathrm{d}^2\mathbf{a}_n(t_{i+2})}{\mathrm{d}t^2} = \lim_{\Delta t\to 0}\frac{\mathbf{a}_n(t_{i+2}) - 2\mathbf{a}_n(t_{i+1}) + \mathbf{a}_n(t_i)}{\Delta t}, \tag{A.7}$$

with the simulation time step $\Delta t = 1$fs and $i = 1, 2, 3, \ldots$. Further, by applying relation (9), one can obtain expressions for the dynamical variables of a higher order. Then, equation (10) can be rewritten in the form adapted for the numerical estimation of the frequency parameters:

$$\Delta_{j+1}^2(k) = \frac{\left\langle\{\mathrm{Re}[A_{j+1}(k,t)]\}^2 + \{\mathrm{Im}[A_{j+1}(k,t)]\}^2\right\rangle}{\left\langle\{\mathrm{Re}[A_j(k,t)]\}^2 + \{\mathrm{Im}[A_j(k,t)]\}^2\right\rangle},$$
$$j = 1,\ 2,\ 3, \ldots. \tag{A.8}$$

For the case of the isotropic equilibrium system, the ensemble average in equation (A.8) is realized by means of the averaging over configurations at different time moments and averaging over different directions of the wavevector **k** at the fixed

$$k = |\mathbf{k}| = \sqrt{k_x^2 + k_y^2 + k_z^2}$$

within the given geometry of the simulation box.

Note that we have verified the various model potentials suggested for liquid lithium. It is remarkable that the pseudopotential proposed by Gonzalez *et al* yields very good agreement with x-ray diffraction data for the structure properties and excellent agreement with IXS data for the dynamical properties [37]. In particular, the scattering intensity $I(k,\omega)$ calculated with this pseudopotential reproduces the experimental data with a higher accuracy than the scattering intensity obtained with the EAM [69] and MEAM potentials [70] (see figure A1). Therefore, we have used this pseudopotential to generate the configuration data and, then, to estimate the frequency parameters.

Thus, the first six frequency parameters $\Delta_1^2(k)$, $\Delta_2^2(k)$, ..., $\Delta_6^2(k)$ of the liquid lithium for the considered wavenumber range were calculated on the basis of molecular dynamics simulation data for the system of $N = 16\,000$ particles interacted through the effective pseudopotential suggested by Gonzalez *et al* [35]. It was employed the cubic simulation box ($L_x = L_y = L_z = 6.98$nm) with the periodic boundary conditions in all the directions. The values of the frequency parameters were also averaged over data of independent simulations runs. The obtained values of these parameters are presented in figure 5.

ORCID iDs

A V Mokshin https://orcid.org/0000-0003-2919-864X
B N Galimzyanov https://orcid.org/0000-0002-1160-5748

References

[1] Resibois P and de Leener M 1977 *Classical Kinetic Theory of Fluids* (New York: Wiley)
[2] Landau L D and Placzek G 1934 *Phys. Z. Sowjun.* **5** 172
[3] Price D L, Saboungi M-L and Bermejo F J 2003 *Rep. Prog. Phys.* **66** 407
[4] Verkerk P 2001 *J. Phys.: Condens. Matter* **13** 7775
[5] Copley J R D and Lovesey S W 1975 *Rep. Prog. Phys.* **38** 461
[6] de Gennes P G 1959 *Physica* **25** 825
[7] Montfrooij W 2016 *J. Non-Cryst. Solids* **445–6** 15
[8] Hansen J P and McDonald I R 2006 *Theory of Simple Liquids* (London: Academic)
[9] Balucani U and Zoppi M 1994 *Dynamics of the Liquid State* (Oxford: Clarendon)
[10] Scopigno T, Ruocco G and Sette F 2005 *Rev. Mod. Phys.* **77** 881
[11] Pilgrim W-C and Chr M 2006 *J. Phys.: Condens. Matter* **18** R585
[12] Egelstaff P A 1965 *Thermal Neutron Scattering* (New York: Academic)
[13] Götze W 1989 Aspects of structural glass transitions *Liquids, Freezing and the Glass Transition* ed J P Hansen *et al* (Amsterdam: North-Holland)
[14] Boon J P and Yip S 1991 *Molecular Hydrodynamics* (New York: Dover)
[15] Ohse R 1985 *Handbook of Thermodynamic and Transport Properties of Alkali Metals* (Oxford: Blackwell Scientific)
[16] Sinn H, Sette F, Bergmann U, Halcoussis C, Krisch M, Verbeni R and Burkel E 1997 *Phys. Rev. Lett.* **78** 1715
[17] Novikov A, Savostin V, Shimkevich A, Yulmetyev R and Yulmetyev T 1996 *Physica* B **228** 312
[18] Copley J R D and Rowe M 1974 *Phys. Rev.* A **9** 1656
[19] Bodensteiner T, Morkel C, Gläser W and Dorner B 1992 *Phys. Rev.* A **45** 5709
[20] Giordano V M and Monaco G 2009 *Phys. Rev.* B **79** 020201
[21] Cabrillo C, Bermejo F J, Alvarez M, Verkerk P, Maira-Vidal A, Bennington S M and Martín D 2002 *Phys. Rev. Lett.* **89** 075508
[22] Torcini A, Balucani U, de Jong P H K and Verkerk P 1995 *Phys. Rev.* E **51** 3126
[23] Casas J, González D J, González L E, Alemany M M G and Gallego L J 2000 *Phys. Rev.* B **62** 12095
[24] Canales M, González L E and Padró J A 1994 *Phys. Rev.* E **50** 3656
[25] Gonzalez D J, González L E and Hoshino K 1994 *J. Phys.: Condens. Matter* **6** 3849
[26] Yulmetyev R M, Mokshin A V, Hänggi P and Yu S V 2001 *Phys. Rev.* E **64** 057101
[27] Yulmetyev R M, Mokshin A V, Hänggi P and Yu S V 2002 *JETP Lett.* **76** 147
[28] Yulmetyev R M, Mokshin A V, Scopigno T and Hänggi P 2003 *J. Phys.: Condens. Matter* **15** 2235
[29] Mokshin A V, Yulmetyev R M and Hänggi P 2004 *J. Chem. Phys.* **121** 7341
[30] Mokshin A V, Yulmetyev R M, Khusnutdinov R M and Hänggi P 2006 *JETP* **103** 841
[31] Anta J A and Madden P A 1999 *J. Phys.: Condens. Matter* **11** 6099
[32] Mokshin A V, Yulmetyev R M, Khusnutdinoff R M and Hänggi P 2007 *J. Phys.: Condens. Matter* **19** 046209
[33] Singh S, Sood J and Tankeshwar K 2007 *J. Non-Cryst. Solids* **353** 3134
[34] Kresse G 1996 *J. Non-Cryst. Solids* **205–7** 833
[35] Gonzalez L E, Gonzalez D J and Lopez J M 2001 *J. Phys.: Condens. Matter* **13** 7801
[36] Salmon P S, Petri I, de Jong P H K, Verkerk P, Fisher H E and Howells W S 2004 *J. Phys.: Condens. Matter* **16** 195
[37] Khusnutdinoff R M, Galimzyanov B N and Mokshin A V 2018 *J. Exp. Theor. Phys.* **126** 83
[38] Scopigno T, Balucani U, Ruocco G and Sette F 2000 *J. Phys.: Condens. Matter* **12** 8009
[39] Singh S and Tankeswar K 2003 *Phys. Rev.* E **67** 012201
[40] Zwanzig R 2001 *Nonequilibrium Statistical Mechanics* (Oxford: Clarendon)
[41] Balucani U, Lee M H and Tognetti V 2003 *Phys. Rep.* **373** 409
[42] Lee M H 2000 *Phys. Rev.* E **62** 1769
[43] Mokshin A V 2015 *Theor. Math. Phys.* **183** 449
[44] Götze W 2009 *Complex Dynamics of Glass-Forming liquids* (Oxford: Oxford University Press)
[45] Vorberger J, Donko Z, Tkachenko I M and Gericke D O 2012 *Phys. Rev. Lett.* **109** 225001
[46] Arkhipov Yu V, Ashikbayeva A B, Askaruly A, Davletov A E and Tkachenko I M 2014 *Phys. Rev.* E **90** 053102
[47] Bhalla P, Dasa N and Singha N 2016 *Physica* A **380** 2000
[48] Ming B Y 2016 *Physica* A **447** 411
[49] Wierling A and Sawada I 2010 *Phys. Rev.* E **82** 051107

[50] Khusnutdinoff R M, Mokshin A V, Klumov B A, Ryltsev R E and Chtchelkatchev N M 2016 *JETP* **123** 265
[51] Chtchelkatchev N M, Klumov B A, Ryltsev R E, Khusnutdinov R M and Mokshin A V 2016 *JETP Lett.* **103** 390
[52] Mokshin A V, Yulmetyev R M and Hänggi P 2005 *Phys. Rev. Lett.* **95** 200601
[53] Yoshido F and Takeno S 1989 *Phys. Rep.* **173** 301
[54] Mountain R D 1966 *Rev. Mod. Phys.* **38** 205
[55] Verkerk P, De-Jong P H K, Arai M, Bennington S M, Howells W S and Taylor A D 1992 *Physica* B **180–1** 834
[56] Burkel E and Sinn H 1994 *J. Phys.: Condens. Matter* **6** A225
[57] Scopigno T, Balucani U, Ruocco G and Sette F 2000 *Phys. Rev. Lett.* **85** 4076
[58] Aliotta F, Gapiński J, Pochylski M, Ponterio R C, Saija F and Vasi C 2011 *Phys. Rev.* E **84** 051202
[59] Bafile U, Guarini E and Barocchi F 2006 *Phys. Rev.* E **73** 061203
[60] Hosokawa S, Pilgrim W-C, Kawakita Y, Ohshima K, Takeda S, Ishikawa D, Tsutsui S, Tanaka Y and Baron A Q R 2003 *J. Phys.: Condens. Matter* **15** L623
[61] Hosokawa S, Kawakita Y, Pilgrim W-C and Sinn H 2001 *Phys. Rev.* B **63** 134205
[62] Bove L E, Sacchetti F, Petrillo C, Dorner B, Formisano F, Sampoli M and Barocchi F 2002 *J. Non-Cryst. Solids* **307–10** 842
[63] Waseda Y 1980 *The Structure of Non-crystalline Materials: Liquids and Amorphous Solids* (New York: McGraw-Hill)
[64] Fomin Yu D, Ryzhov V N, Tsiok E N, Brazhkin V V and Trachenko K 2016 *J. Phys.: Condens. Matter* **28** 43LT01
[65] Touioukiam Y and Ho C 1973 *Thermal Diffusivity* (*Thermophysical Properties of Matter* vol 10) (New York: IFI-Plenum)
[66] Giordano V M and Monaco G 2010 *Proc. Natl Acad. Sci.* **107** 21985
[67] Hosokawa S, Inui M, Kajhara Y, Tsutsui S and Baron A Q R 2015 *J. Phys.: Condens. Matter* **27** 194104
[68] Reichman D R and Charbonneau P 2005 *J. Stat. Mech.* P05013
[69] Belashchenko D K 2012 *Inorg. Mater.* **48** 79
[70] Baskes M I 1992 *Phys. Rev.* B **46** 2727